Fusion pores and their control of neurotransmitter and hormone release

Che-Wei Chang, Chung-Wei Chiang, and Meyer B. Jackson

Department of Neuroscience, University of Wisconsin–Madison, Madison, WI 53705

Ca^{2+}-triggered exocytosis functions broadly in the secretion of chemical signals, enabling neurons to release neurotransmitters and endocrine cells to release hormones. The biological demands on this process can vary enormously. Although synapses often release neurotransmitter in a small fraction of a millisecond, hormone release can be orders of magnitude slower. Vesicles usually contain multiple signaling molecules that can be released selectively and conditionally. Cells are able to control the speed, concentration profile, and content selectivity of release by tuning and tailoring exocytosis to meet different biological demands. Much of this regulation depends on the fusion pore—the aqueous pathway by which molecules leave a vesicle and move out into the surrounding extracellular space. Studies of fusion pores have illuminated how cells regulate secretion. Furthermore, the formation and growth of fusion pores serve as a readout for the progress of exocytosis, thus revealing key kinetic stages that provide clues about the underlying mechanisms. Herein, we review the structure, composition, and dynamics of fusion pores and discuss the implications for molecular mechanisms as well as for the cellular regulation of neurotransmitter and hormone release.

The Journal of General Physiology

Introduction

The packaging of signaling molecules into vesicles gives exocytosis an intrinsically quantal character. In its simplest form, the fusion of a vesicle with the plasma membrane can be viewed as complete and instantaneous. Very rapid release can raise the concentration of a signaling molecule to high levels around the release site at the cell surface, creating an extremely steep gradient that collapses rapidly as signaling molecules spread out by diffusion. However, release is often graded and slow; a vesicle can release a variable portion of its content over an extended period of time. Partial release makes exocytosis subquantal, and slow release keeps the extracellular concentration from getting very high. Furthermore, most secretory vesicles contain multiple signaling molecules that may be released in different proportions and at different rates depending on the triggering signal.

The speed with which signaling molecules are secreted is determined by the fusion pore, which provides a narrow aqueous connection from the vesicle lumen to the extracellular space. As essential kinetic intermediates of membrane fusion, fusion pores are the natural object of studies of molecular mechanisms. For these reasons, fusion pores have been the subject of intense interest for many years (Monck and Fernandez, 1994; Lindau and Almers, 1995; Lindau and Alvarez de Toledo, 2003; Harata et al., 2006; Jackson and Chapman, 2008; Sørensen, 2009; Vardjan et al., 2009). A fusion pore must be quite narrow when it first forms, but it can expand to allow the vesicle membrane to merge with the plasma membrane. Tuning exocytosis can be achieved by stabilizing the pore in an intermediate state, by grading the speed of fusion pore expansion, by shrinking the fusion pore, or by closing the fusion pore to recover and recycle the vesicle. Synapses can achieve submillisecond speed and precise timing by opening and expanding fusion pores rapidly. In contrast, endocrine functions rarely depend on rapid release. Hormone diffusion through tissue, organ, or organism can take seconds or longer, so nothing is lost by spreading exocytosis out over time scales of hundreds of milliseconds or seconds. Endocrine release is tailored for flexibility and control; synaptic release is tailored for speed. Both neurons and endocrine cells use a canonical molecular complex (Walch-Solimena et al., 1993; Martin, 1994), and it is fascinating that this basic complex can be adapted to such a wide range of functions.

Distinct functional needs translate into requirements for fusion pores with specific structures, permeabilities, and dynamic behavior. This article presents current knowledge about fusion pores with an emphasis on their molecular composition, dynamic transitions, and functional roles. Clues about fusion pores come from many sources, and a wide range of experimental approaches have provided glimpses into different aspects and properties. We will survey fusion pore structure, composition, and dynamics and emphasize the diversity of forms and behavior. Wherever possible, we will discuss the molecular basis and functional implications of fusion pore properties and diversity. Finally, we present a detailed analysis of synaptic release to illustrate the impact of pore state on biological function.

Correspondence to Meyer B. Jackson: mbjackso@wisc.edu
Abbreviation used: TMD, transmembrane domain.

The Rockefeller University Press $30.00
J. Gen. Physiol. 2017 Vol. 149 No. 3 301–322
https://doi.org/10.1085/jgp.201611724

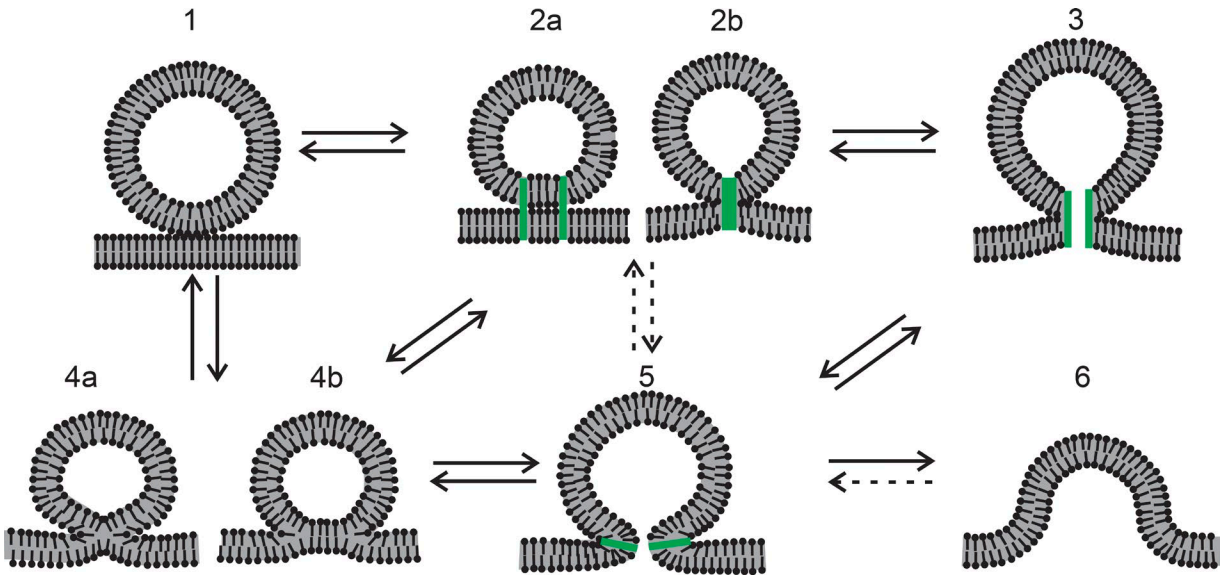

Figure 1. **Putative intermediates of membrane fusion and their transitions.** Transitions that are less relevant or speculative are indicated by dashed arrows. Protein elements are colored green. (1) A vesicle approaches the plasma membrane. (2) Proteins hold the vesicle and plasma membrane together, either through separate contacts (a) or through one central contact (b). (3) A proteinaceous fusion pore could form from a central contact as in 2b. (4) Lipid mixing of the outer (proximal) leaflets can begin, first through the formation of a stalk (4a) and then through the formation of an extended hemifusion diaphragm (4b) in which the fused proximal leaflets retract and leave a bilayer formed by the two distal leaflets. (5) A fusion pore formed by a contiguous lipid bilayer curved into an hourglass-like shape. (6) A greatly expanded lipid fusion pore on the way to complete merger of the plasma and vesicle membranes.

The fusion landscape

Fusion pores should be viewed within the broader framework of mechanisms of exocytosis. To fuse, a vesicle must contact the plasma membrane, and this contact must undergo structural transitions. Fig. 1 illustrates the key intermediates that have been invoked, starting with a vesicle touching the plasma membrane (state 1). A contact becomes more intimate by establishment of a protein connection in which the proteins could be separate (state 2a) or associated (state 2b). State 2b could be viewed as a closed fusion pore, which could open to a proteinaceous pore (state 3). These structures require transmembrane domains (TMDs) of proteins in the vesicle and plasma membrane. A connection represented in state 2 could also evolve to a lipid stalk (state 4a), which can expand to a hemifusion diaphragm (state 4b). A lipidic fusion pore (state 5) is an essential intermediate in any model of membrane fusion, and its immediate precursor could be either state 3 or state 4b, or possibly even state 2, although this last route is more speculative. In a lipidic pore, the two membranes have fused, but the process is actually not complete at this point. Full merger to a single flat membrane requires that the lipidic pore expand (state 6). Possible transitions between these various states are indicated by arrows in Fig. 1, and most of these transitions are thought to be reversible. Expansion of state 5 to state 6 can also be reversed by a budding process performed by membrane curvature–inducing proteins, but reversal at this stage is irrelevant to the present focus. States 3 and 5 are fusion pores, and states 2 and 4 can become fusion pores. So fusion pores are where the action is with regard to mechanistic studies. The landscape illustrated in Fig. 1 serves as a useful road map to the present discussion, and experimental studies of fusion can be interpreted in terms of these hypothesized structures.

Structure

There have been many attempts to use electron microscopy to observe the initial steps of fusion during exocytosis. The smallest pores captured between fusing vesicles and the plasma membrane have diameters of 8–20 nm (Chandler, 1991). Freeze fracture images show pores with a range of shapes and possibly without particles (no protein). There can be little doubt that even the smallest of these pores seen in the electron microscope consist of a contiguous lipid bilayer that curves smoothly to join the two fusing membranes (Fig. 1, state 5). However, the initial fusion pores inferred from conductance measurements must be smaller, with diameters <1 nm (discussed below in Transport properties–Fusion pore conductance). Whether these pores are composed of lipid bilayer (Fig. 1, state 5) or protein (Fig. 1, state 3) remains unresolved.

Stimulation of synapses or endocrine cells generally induces fusion of only a small fraction of the available vesicles, so fusion pores are rare kinetic intermediates. This together with generally short lifetimes makes it especially difficult to capture fusion pores for struc-

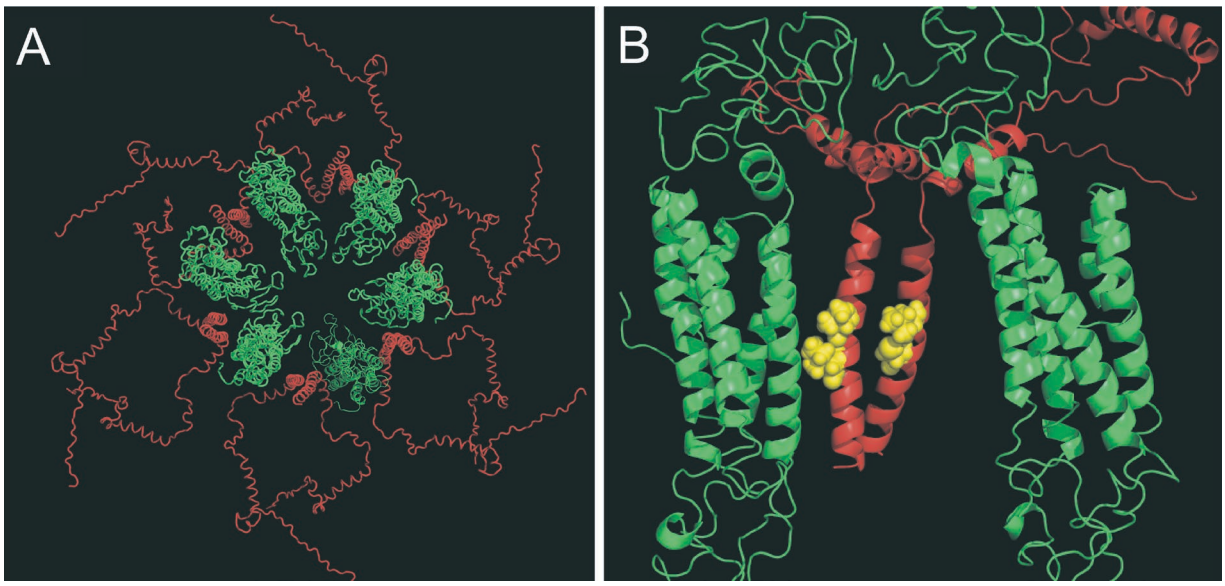

Figure 2. **A structural model of a synaptophysin–synaptobrevin complex.** The model was based on a study by Adams et al. (2015) and generated with PyMOL using a pdb file provided by M. Stowell. (A) The complete complex viewed from the vesicle lumen shows 6 synaptophysins (green) and 12 synaptobrevins (red) in a hexagonal formation. 12 synaptophysin TMDs and 12 synaptobrevin TMDs face inward and could line a fusion pore. (B) The TMDs of two synaptophysin and two synaptobrevin molecules are viewed from within the plane of the membrane. Residues highlighted in yellow were implicated as pore liners by amperometry experiments with synaptobrevin TMD mutants (Chang et al., 2015); synaptobrevin residues 99 and 103 are highlighted on one chain, and residues 101 and 105 are highlighted on the other (compare with Fig. 4 B).

tural work, and there are no structures of initial fusion pores from biological samples. So far, what little structural insight we have of early-stage pores was derived from studies of model systems with defined chemical compositions. The vesicle proteins synaptophysin and synaptobrevin associate into hetero-oligomers, and these complexes have been purified and studied with negative stain electron microscopy. Because one of the TMDs of synaptophysin is homologous to a connexin TMD, the gap junction Cx26 crystal structure was used to build a model in which 6 synaptophysin molecules and 12 synaptobrevin molecules form a ring-like arrangement (Fig. 2 A). The relevance of this structure to exocytosis remains unclear, but it has remarkable parallels with a model based on amperometric measurements of fusion pore flux in cells expressing synaptobrevin TMD mutations (Fig. 4 B). The model of the synaptobrevin–synaptophysin complex places synaptobrevin in two different configurations, with TMDs oriented differently relative to the pore axis. Of the four residues of the synaptobrevin TMD implicated as pore liners by amperometry (Chang et al., 2015), two face into the pore lumen for one of the synaptobrevins in the structure, and the other two residues face into the lumen in the other synaptobrevin in the structure (Fig. 2 B).

The model in Fig. 2 suggests that synaptophysin forms part of the fusion pore. Synaptophysin forms channels in lipid bilayers (Thomas et al., 1988), but a function in fusion pores was thought to be unlikely when a synaptophysin knockout was shown to have normal synaptic release (McMahon et al., 1996). Without synaptophysin, synapses have slower endocytosis (Kwon and Chapman, 2011), and in endocrine cells, synaptophysin–dynamin interactions modulate release at a step downstream from the initial fusion pore (González-Jamett et al., 2010). However, genetic studies with synaptophysin are complicated by the presence of three homologous proteins that could substitute for synaptophysin (Arthur and Stowell, 2007). Recent amperometry experiments in chromaffin cells have demonstrated that molecular manipulations of synaptophysin produce significant changes in fusion pore properties (unpublished data).

Although the synaptophysin–synaptobrevin model in Fig. 2 is intriguing, it implies a pore that is too large. A total of 24 TMDs line the putative pore, including 12 molecules of synaptobrevin. Estimates of the number of SNARE molecules required for fusion vary widely but are generally much lower (discussed below in Composition–SNARE number). Fusion pore conductance measurements (also discussed below in the same section) indicate that the pore could be lined by as few as five to eight TMDs. This makes it unlikely that the structure in Fig. 2 forms the initial fusion pore of exocytosis. However, the parallel with amperometry results are intriguing, and the capacity of synaptobrevin and synaptophysin TMDs to come together is probably relevant. If the TMD–TMD interfaces between these two proteins are

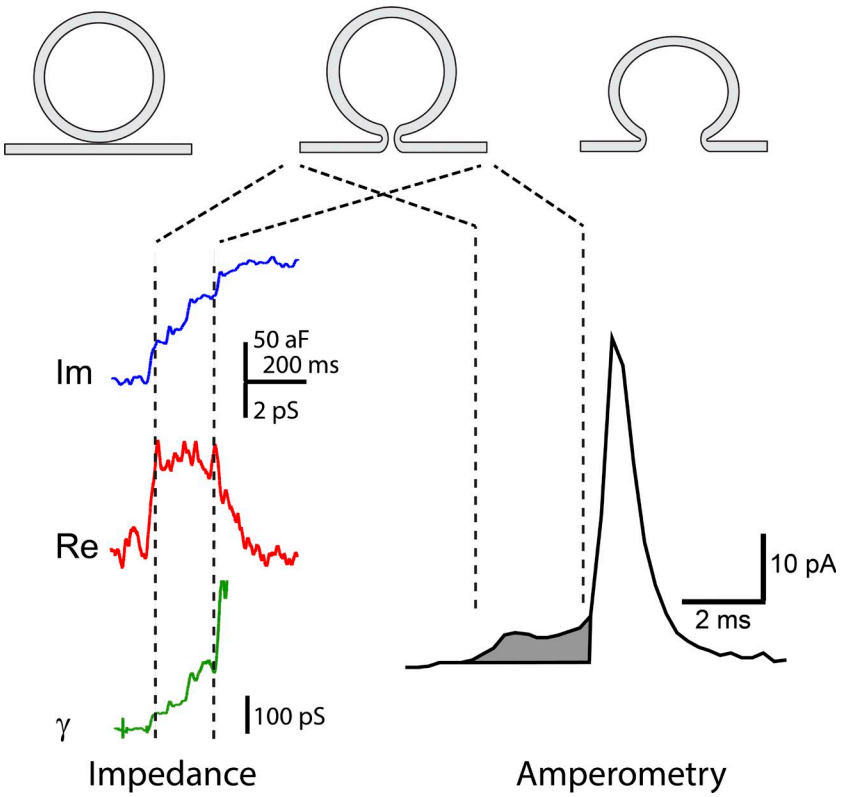

Figure 3. **Impedance and amperometry measurements of fusion pores can be interpreted in terms of three successive stages of membrane fusion.** (1) Contact (top left), (2) fusion pore opening (top middle), and (3) fusion pore expansion (top right). (left) Impedance recording reveals fusion pore openings as a change in the complex impedance of a patch of membrane to which a vesicle fuses. The imaginary component of the impedance (blue) and real component (red) are used to calculate the fusion pore conductance, γ (green; Lollike et al., 1995). The opening of a fusion pore produces an initial conductance increase, and fusion pore expansion increases the conductance further. (right) Amperometry recording reveals a fusion pore opening as a pre-spike foot (shaded), which represents the flux of catecholamine out of the vesicle at a limited rate. Fusion pore expansion allows content release much more rapidly to produce an amperometric spike.

flexible, then smaller complexes and pores with fewer TMDs may be possible.

Transport properties

A fusion pore provides a conduit for transport, and most of what we know about fusion pores derives from measurements of some form of flux. Ions and signaling molecules can flow through the aqueous pore lumen, and membrane can flow along the pore walls. The transport of ions, signaling molecules, and membrane can be measured and used to gain insight into fusion pore structure and composition. Fig. 3 illustrates how patch clamp measurements of conductance and amperometry measurements of content flux signal the evolution of the fusion pore. These two techniques both report a nascent pore that supports low but detectable transport. Each measurement reveals a sequence of steps beginning with pore opening and continuing with pore expansion.

Fusion pore conductance. Fusion pore conductance can be determined with various electrical recording configurations (Breckenridge and Almers, 1987; Zimmerberg et al., 1987; Lindau and Neher, 1988; Lindau and Alvarez de Toledo, 2003). One must measure the complex impedance of a membrane and interpret the results with the aid of an equivalent circuit consisting of a fusing vesicle and its pore in parallel with a patch of membrane. An initial increase in conductance concomitant with an increase in capacitance provides information about the nascent fusion pore, and ensuing increases provide a readout of the progress of fusion over time (Fig. 3).

Fusion pore conductance is related to pore geometry, and the simplest way to envisage this relationship is to hypothesize that a fusion pore behaves like the solution that fills it. This involves using the macroscopic expression for the conductance, γ, of an element of solution. A pore with length, *l*, and constant cross-sectional area, *A*, has a conductance of

$$\gamma = \frac{A}{\rho l}. \quad (1)$$

ρ is the resistivity of the aqueous solution filling the pore (ρ ~100 Ω cm for standard physiological saline). It is common to take *l* as roughly twice the thickness of a lipid bilayer (~10 nm). If the pore is cylindrical with radius *r*, then *A* is πr^2, and we can use the conductance to estimate *r*. This expression has been tested with ion channels, and with γ ~1 nS, calculations with Eq. 1 using structural estimates of *A* and *l* give conductance values roughly three times higher than experimental measurements (Jackson, 2006). The error is much larger for smaller channels. The main reason for this discrepancy is that Eq. 1 neglects interactions between the ions and the walls of the pore and surrounding membrane. Actual fusion pores are likely to be wider than estimates based on conductance, so Eq. 1 provides a lower limit for *r*. One might hope to have more confidence in Eq. 1 for very high conductances, but then another prob-

lem arises: the conductance of the approach to the pore must be included. Eq. 1 then must incorporate an additive term that is proportional to *r* rather than *A* (Hille, 1992; Nanavati et al., 1992; Jackson, 2006).

Despite the reservations just discussed regarding the quantitative dependence of conductance on radius, the wide range of values for fusion pore conductance indicates that fusion pore sizes also vary. Conductances vary by over two orders of magnitude, ranging from ~20 pS (Klyachko and Jackson, 2002) to several nanosiemens (Monck et al., 1990; Spruce et al., 1990; Nanavati et al., 1992; Curran et al., 1993). Thus, pore radii may vary by roughly one order of magnitude. In the same patch of membrane of nerve terminals, fusion of small synaptic-like vesicles and large dense-core vesicles have fusion pore conductances differing by a factor of ~10 (Klyachko and Jackson, 2002). The large conductances of endocrine fusion pores have been interpreted in terms of a lipidic pore (Fig. 1, state 5) using a continuum elasticity model based on the mechanical properties of lipid bilayers (Nanavati et al., 1992). Vesicles fusing with membranes in the absence of proteins produce pores with large conductances that fluctuate very widely (Chanturiya et al., 1997). Theoretical work on the shape of fusion pores formed by an elastic lipid bilayer suggests that their radii range from 1.1 to 4.2 nm (Jackson, 2009). Pores of this size should have conductances in the nanosiemens range. So larger fusion pore conductances are consistent with the elastic properties of a lipid bilayer, but smaller fusion pore conductances are not. Smaller pores are therefore less likely to be purely lipidic. Conductances overlapping with the range of ion channels was one of the earliest arguments for a proteinaceous pore (Almers, 1990; Lindau and Almers, 1995; Lollike et al., 1995). Furthermore, ion channel conductances generally do not fluctuate much, so the greater stability of small conductance fusion pores points to a proteinaceous structure.

Content flux. Amperometry provides the most sensitive measurement currently available for flux of vesicle content through a fusion pore. This electrochemical technique detects readily oxidized molecules contained in many vesicles such as catecholamines, histamine, dopamine, and serotonin. The loss of content from a single vesicle is readily observed (Wightman et al., 1991), and a single-vesicle release event progresses through distinct stages. First comes the "pre-spike foot" that reports flux through an initial fusion pore (shaded region of the amperometry trace in Fig. 3; Chow et al., 1992; Jankowski et al., 1993). The spike comes next when the pore starts to expand. Kiss-and-run exocytosis also is accompanied by flux through a fusion pore (Alvarez de Toledo et al., 1993; Wang et al., 2003, 2006), and the implications for pore closure are discussed below (Dynamic properties–Closure).

Because vesicles often contain multiple signaling molecules with different sizes, fusion pores can act as filters to select which molecules will pass. The molecules detected by amperometry are generally small with molecular masses <200 D. Permeation of the initial pore by molecules of this size fits with the ~1-nm dimensions of pores inferred from conductance measurement. The vesicles of pancreatic β cells contain ATP and GABA and can be loaded with exogenous serotonin. By expressing $GABA_A$ receptors and purinergic P_2X_2 receptors, the release of ATP and GABA can be monitored as an ion current through the plasma membrane (Braun et al., 2007). ATP, GABA, and serotonin all were found to pass through the initial fusion pore during β cell exocytosis, but at different rates. The flux was greatest for the smallest molecule, GABA, and lowest for the largest molecule, ATP, consistent with a filtering action by an ~1.4-nm pore. *N*-methyl-D-glucamine is also small and should pass through fusion pores easily, but passage of this molecule could not be seen in pores formed during SNARE-mediated fusion of nanodiscs with cells (Wu et al., 2016). These fusion pores may be different from dense-core vesicle fusion pores, but it is also possible that factors other than size have an impact on permeability.

The most pronounced filtering appears with peptides, both between different sized peptides and between peptides versus smaller molecules. As soon as a fusion pore opens it allows pH to equilibrate, but vesicles begin to lose their peptides with a delay of about a second after pH equilibration (Barg et al., 2002; Tsuboi and Rutter, 2003). The smaller peptide neuropeptide Y is released very rapidly, and the larger peptide tissue plasminogen activator is released very slowly, even when the two are contained in the same vesicle (Perrais et al., 2004). The vesicles of chromaffin cells contain both catecholamine and large peptide hormones. Chromaffin cells release norepinephrine in response to weak stimulation, but stronger stimulation elicits release of both catecholamine and the large peptide chromogranin (Fulop et al., 2005). Thus, with weak stimulation the fusion pore remains in its initial narrow state, and strong stimulation drives its expansion to a wider state. Likewise, stronger stimulation of β cells triggers fusion pore expansion to allow insulin release (MacDonald et al., 2006). In lactotrophs, weak stimulation opens a small pore that only allows pH to equilibrate, whereas stronger stimulation allows larger fluorescent tracers to pass (Vardjan et al., 2007). These various experiments suggest that pore size is a critical determinant in selecting which signaling molecules are secreted and that the mode of release depends on the form of stimulation. However, as a cautionary note, it was found that subtle variations in the structures of fluorescently tagged peptides had a profound impact on release kinetics (Michael et al., 2004). These results cannot be explained by

filtering of molecules with different sizes and suggest an influence of other factors such as interactions between the released molecule and the vesicle matrix.

Content flux and conductance. When content flux and conductance are measured in parallel, the two quantities show a tight correlation. In mast cells, as the fusion pore expanded, serotonin flux increased in proportion with measured conductance. But the flux was much lower than a theoretical estimate based on the pore radius and conductance (Alvarez de Toledo et al., 1993). Using patch amperometry (Albillos et al., 1997) to measure catecholamine flux and conductance simultaneously, the two quantities were found to vary in parallel over a wide range, with a flux of 2.2×10^7 molecules s^{-1} nS^{-1} (Gong et al., 2007). This work suggested that fusion pores show little if any selectivity between cations, but the status of anion permeability could not be assessed. These results fit with a general correlation between ion conduction and content flux. Thus, even without knowing the actual dimensions of a fusion pore, it is reasonable to assume that higher conductance fusion pores will permit more rapid release of content and that lower conductance pores will preferentially release smaller molecules.

Membrane flux. A fluorescent dye that partitions into lipid bilayers should move between the vesicle and plasma membrane in a lipidic fusion pore (Fig. 1, state 5) but not a proteinaceous fusion pore (Fig. 1, state 3). Early attempts to test this idea to study viral fusion suggested that the smallest fusion pores do not allow lipid flow (Tse et al., 1993), but theoretical analysis suggests that detecting this flux in small pores could be very challenging (Chizmadzhev et al., 1999). In endocrine cells, single-vesicle fluorometry showed that during a kiss-and-run event a lipid marker was lost without the loss of a fluorescent-tagged protein (tissue plasminogen activator) contained in the vesicle (Taraska and Almers, 2004). This indicated the presence of a lipidic pathway through the lining of a pore that was large enough to pass an organic fluorophore but not large enough to pass a protein. This suggests that this pore is lipidic and further makes the important point that such a structure can close. A plasma membrane lipid label was observed to move to the vesicle membrane before the passage of a water-soluble fluorescent dye into the vesicle lumen and before the equilibration of vesicle pH (Zhao et al., 2016). This indicates that lipid contact is established before pore opening. This result supports fusion through the formation of a hemifusion intermediate (Fig. 1, state 4) or a composite protein–lipid pore in which the proximal leaflets are connected (discussed below; Fig. 9).

Single-vesicle capacitance measurements can detect changes in the area of a vesicle as membrane moves through a fusion pore. As long as fusion pores are small, there is no detectible loss of membrane; the capacitance remains flat, and up-steps are tightly correlated with the down-steps (Lollike et al., 1998; Klyachko and Jackson, 2002). When a fusion pore's conductance exceeds ∼1 nS, the down-step can be smaller than the up-step, indicating that some membrane has flowed through the rim of the fusion pore from the vesicle to the plasma membrane (Monck et al., 1990). Thus, capacitance recording shows that membrane flows through large fusion pores but not small fusion pores. This suggests a general trend that small pores are made of protein and large pores are made of lipid. However, the absence of membrane flux in capacitance recording is difficult to square with the early stage movement of fluorescent membrane label just mentioned (Zhao et al., 2016).

Composition

The molecular components that make up the fusion pore have been difficult to identify. Models have been proposed of fusion pores composed of protein or lipid, and these views are widely held to be mutually exclusive. In the absence of high-resolution structures, efforts to determine what fusion pores are made of have relied on indirect measurements.

SNARE TMDs. Early work on SNARE-mediated fusion demonstrated a functional role for SNARE TMDs in membrane trafficking (Grote et al., 2000). SNAREs with a TMD replaced by a lipid anchor can support fusion of reconstituted proteoliposomes provided that the lipid is long enough to span the entire bilayer or there are multiple acyl groups attaching a SNARE to the membrane (McNew et al., 2000). Fusion of yeast vacuoles can occur with some lipid-anchored SNAREs but not others (Pieren et al., 2015). In another study in yeast vacuoles, lipid-anchored SNAREs supported lipid mixing provided that three accessory proteins were present (Xu et al., 2011). One study claimed that lipid-anchored SNAREs are fully functional in synaptic release and that synaptobrevin worked as well as wild type when its TMD was replaced by a domain from CSPα with 13 lipid acylation sites (Zhou et al., 2013). However, the wild-type synaptobrevin construct used in this study was subsequently shown to be defective (Chang et al., 2016; Dhara et al., 2016). Wild-type synaptobrevin supported release to levels approximately fourfold higher than the CSPα-synaptobrevin construct. Anchoring synaptobrevin with motifs harboring one or two lipid acyl groups failed to increase release above the background level of neurons from a synaptobrevin/cellubrevin double knockout (Chang et al., 2016). The result with the CSPα construct suggests a weak fusion capability of a SNARE lacking a TMD, and thus argues against a proteinaceous pore. However, it should be kept in mind that the C-terminal segment from CSPα may be long enough to form a

TMD and harbors potential TMD sequences. Furthermore, the large number of lipid acyl groups concentrated into a small segment of protein could reshape lipid bilayers in ways that are difficult to predict. In vitro assays with the synaptobrevin-CSPα construct indicate that its capacity for lipid mixing (Chang et al., 2016) occurs without content mixing (Bao et al., 2016), so it does not form a fusion pore, and the fusion observed in cells may depend on other proteins (e.g., synaptophysin). These results do not rule out the possibility for some fusion mediated by SNAREs anchored to a membrane by lipid rather than a TMD. However, to achieve the level of exocytosis seen with wild-type SNAREs in synapses and endocrine cells, TMDs are required (Chang et al., 2016).

Measurements of catecholamine flux through fusion pores have implicated SNARE TMDs as structural components. The amplitudes of pre-spike feet from amperometry recordings can be modulated by mutations in the TMDs of syntaxin (Han et al., 2004; Han and Jackson, 2005) and synaptobrevin (Chang et al., 2015). Residues with large side chains reduced flux, and residues with small side chains increased flux. Residues with positive or negative charge altered fusion pore flux in a manner consistent with an electrostatic interaction between the TMD and catecholamine. Selected mutants altered pore conductance in a consistent manner. The residues influencing flux fell on one helical face of the syntaxin TMD and on two helical faces of the synaptobrevin TMD. Synaptobrevin with its entire TMD replaced by valines, leucines, or isoleucines supported exocytosis in endocrine cells and the pre-spike feet were altered in a manner consistent with changes in side chain size (Dhara et al., 2016). By analogy with a large body of mutagenesis work on ion channel permeation, these studies supported a model of a fusion pore as a barrel-like structure lined by SNARE TMDs (Fig. 1, state 3).

In vitro experiments with lipid vesicles and nanodiscs showed that TMD residues become accessible to water during fusion (Bao et al., 2016). Mutations of some of the same residues also altered glutamate flux through fusion pores, but the correspondence between water accessibility and glutamate flux was not perfect (Fig. 4 A). Some of the syntaxin TMD residues that influenced glutamate flux also influenced the amperometric pre-spike foot, but other residues of the syntaxin TMD that influenced glutamate flux did not. However, these residues were accessible to an aqueous label. Two of the synaptobrevin TMD residues that influenced the amperometric pre-spike foot also influenced glutamate flux and were water accessible, but two others were not. Thus, there was some correspondence with the residues that influence flux through endocrine vesicles (Han et al., 2004; Chang et al., 2015), but this correspondence was not perfect. Fig. 4 A summarizes these various results. The residues implicated as pore liners generally fell along helical faces of the TMD, but the differences between residues implicated in the various assays may mean that the TMDs are pliable and can form pores in different orientations. This may be related to fusion pore formation with different numbers of SNAREs, or TMDs from other proteins, or variable amounts of lipid. However, the disparate results may also mean that there are more complicated structures beyond the reaches of current thinking.

Based on the locations of the residues that influence fusion pore flux and conductance in endocrine cells, a model was proposed for a proteinaceous fusion pore (Fig. 1, state 3) formed by the SNARE TMDs (Fig. 4 B). The two faces of the synaptobrevin TMD presumably alternate, placing half of the synaptobrevins in one environment and the other half in another environment. This feature parallels the dual arrangement of synaptobrevin TMDs in the structure of the synaptophysin–synaptobrevin complex determined by electron microscopy (Fig. 2; Adams et al., 2015). It is interesting that the cellular assay with amperometry implicated a helical face not seen in the in vitro assays (Fig. 4 A). This may mean that this face can only become a pore liner in the presence of synaptophysin (Fig. 2). In summary, a structural role for TMDs is supported by flux measurements in cells, flux and chemical labeling in vitro, and a structural model. This convergence of results from very different experimental approaches strengthens the case for TMDs as structural components of fusion pores.

SNARE number. There have been many attempts to determine the number of SNARE complexes required for fusion, and these numbers vary widely. To form a channel surrounded by TMDs requires multiple copies, and by analogy with ion channels, this suggests that a fusion pore would need at least four TMDs through each membrane. Because syntaxin and synaptobrevin each have one TMD, this places a requirement of four SNARE complexes. As discussed above (Transport properties–Fusion pore conductance), fusion pore conductance provides an estimate of size, and using a radius of 0.35 nm for a generic α-helix, the conductance measurements from endocrine fusion pores yield an estimate of 5–10 TMDs through each membrane (Han et al., 2004; Zhang et al., 2010b). However, as noted in the discussion of the validity of Eq. 1 above, the actual radius is probably larger than that calculated from conductance.

There are more direct ways to estimate SNARE number. Single molecule photometric counting suggests that only two molecules of synaptobrevin are sufficient for synaptic release (Sinha et al., 2011). Fusion depends on the number of functional SNAP-25 molecules raised to the third power, suggesting that endocrine release requires at least three SNARE complexes (Hua and

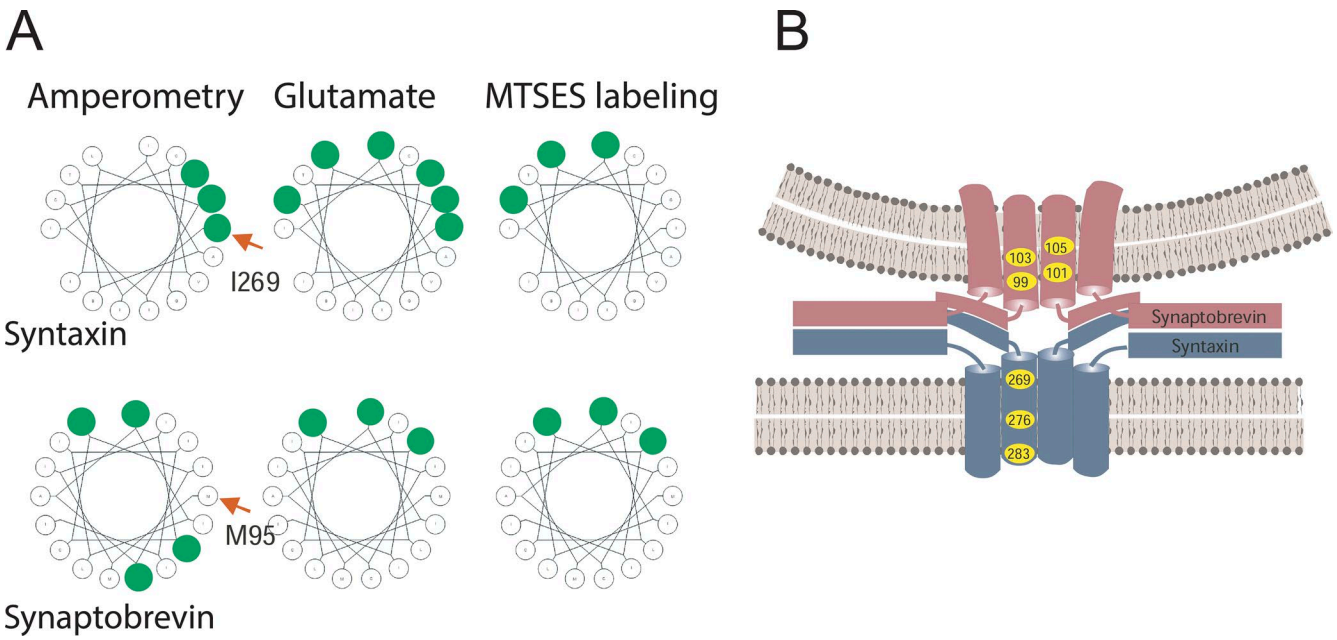

Figure 4. **SNARE TMD residues lining the fusion pore.** (A) Residues in the SNARE TMDs identified by various fusion pore measurements are highlighted in green. The first TMD residue of the wheel is labeled with a red arrow. Amperometry identified some residues (Han et al., 2004; Chang et al., 2015). Glutamate flux and labeling by MTSES identified some of the same residues as well as some different residues (Bao et al., 2016). Many of the residues identified in a given assay fell along one face of a helical wheel (wheels generated at http://kael.net/helical.htm). (B) Fusion pore model based on TMD mutagenesis and amperometric pre-spike feet and conductance in endocrine release (Chang et al., 2015).

Scheller, 2001; Mohrmann et al., 2010). Experiments on fusion in reconstituted systems suggest minimal numbers as low as one (van den Bogaart et al., 2010) or as high as 9 (Domanska et al., 2010). One SNARE complex may be sufficient for pore formation, but pore expansion requires three complexes (Shi et al., 2012). Measurement of content loss by liposomes fusing with nanodiscs suggests the minimum is two (Bao et al., 2016), and these authors suggested that the fusion pore is composed of both protein and lipid.

Lipid. Flux of fluorescent lipid tracer (Taraska and Almers, 2004; Zhao et al., 2016), large sizes, large fluctuations (Spruce et al., 1990; Curran et al., 1993), and membrane loss (Monck et al., 1990) all suggest a contiguous lipidic pathway from the vesicle to the plasma membrane (Fig. 1, state 5). In some cases, these observations could represent a later state of pore evolution rather than the initial state, but the most recent of these studies detected lipid flow before pH equilibration as detected by pHluorin within the vesicle (Zhao et al., 2016). This indicates that lipid connectivity is achieved before the formation of an aqueous pore. TMD mutagenesis studies and content flux measurements do not rule out the presence of lipid, as originally acknowledged (Han et al., 2004). However, a purely lipidic pore is difficult to reconcile with the results summarized above on TMD mutagenesis (preceding section). The observation of smaller amplitude amperometric pre-spike feet with a truncated form of SNAP-25 has been interpreted as evidence for both protein and lipid in the fusion pore (Fang et al., 2008), but there are other possible explanations, such as a reduction in the number of SNARE complexes and SNARE TMDs. As just noted, the presence of both lipid and protein has also been proposed based on liposome-nanodisc fusion studies (Bao et al., 2016). This may be the only way to reconcile prior lipid flux and small numbers of SNAREs with TMD mutant effects. Plausible models for a composite lipoprotein fusion pore have received little attention and will be discussed below (Fig. 9).

A continuum elasticity model of lipidic fusion pores yielded structures with minimum energies in which pore diameters ranged from 1.1 to 4.2 nm (Jackson, 2009). This range fits well with late-stage fusion pores but is difficult to reconcile with the smallest conductances of <100 pS observed in several studies (discussed above in Transport properties–Fusion pore conductance). A study of fusion pore expansion proposed that a lipidic fusion pore with highly curved lipid bilayer could form from a proteinaceous pore in which there is very little bending of lipid bilayers. This idea was proposed to account for the observation that large vesicles have pre-spike feet with longer lifetimes than small vesicles (Zhang and Jackson, 2010). To interpret this relationship, a model was developed based on the notion that a lower area of curved membrane will form in a fusion pore formed by a small lipidic

vesicle (Fig. 5 A). This model recapitulated the dependence of pre-spike foot duration on vesicle size, predicting that the logarithm of one over fusion pore lifetime varies as one over the cube root of the vesicle content (Fig. 5, C and D). Furthermore, the slope of this relation depends on the spontaneous curvature of the lipid bilayer. Perturbing bilayer curvature with cone-shaped and inverted cone-shaped lipids altered this dependence in the manner predicted by the model (Fig. 5 C). Cholesterol removal also accelerated the transition from pre-spike foot to spike, which could be explained by easing the bending of membranes (Wang et al., 2010). Perturbing the lipid bilayer curvature with mutations in the synaptobrevin TMD also altered the dependence of pre-spike foot duration on vesicle size (Fig. 5 D; Chang and Jackson, 2015). Tryptophan substitutions could alter the relation in different ways depending on their location within the membrane. These results indicated that the fusion pore of the amperometric pre-spike foot forms without significant bending of membranes and thus supported the hypothesis of an initial proteinaceous structure. Fusion pore formation entails little membrane bending, and it is the subsequent expansion step that must overcome a significant elastic energy barrier to bend lipid bilayers into the shape of a pore (Fig. 1, state 5). Progression from a pre-spike foot to a spike in amperometry recordings could thus entail a transition from state 3 to state 5 of Fig. 1.

Dynamic properties

Closure. The earliest single-vesicle capacitance recordings showed that stepwise capacitance increases were often followed by stepwise capacitance decreases within ~1 s (Neher and Marty, 1982; Fernandez et al., 1984). Amperometry measurement of the flux of a vesicle's content through a fusion pore revealed abrupt openings followed by abrupt closings (Alvarez de Toledo et al., 1993; Zhou et al., 1996; Wang et al., 2003, 2006). Fluorescent tracer loss from vesicles can be partial, suggesting the termination of release by pore closure (Aravanis et al., 2003; Richards et al., 2005). Thus, three different kinds of measurement suggest that a vesicle can lose content without collapsing into the plasma membrane. This so-called kiss-and-run form of release implies that fusion pores have the capacity to close. Pore closure creates two scenarios. In one case, the pore closes by a simple reversal of the opening transition, like the reversible gating of an ion channel. In the other scenario, an initial pore closes by a route distinct from the initial opening transition, perhaps with a transition to another open state that then closes. The first case is thermodynamically reversible and restores a vesicle to its initial ready-to-open state. The second case would leave a vesicle in a different state from where it started. These irreversible transitions are more likely to end with a closed pore not necessarily capable of producing further openings.

Rapid successions of repeated openings and closings, or flickers (Henkel et al., 2000), suggest a reversible protein conformational change, represented by transitions between state 2 and state 3 in Fig. 1. The brief time interval between the upward and downward steps suggests tight coupling, as would be the case if pore closing is a simple reversal of pore opening. The rapid repeated openings mean that these closures restore a vesicle to a ready-to-open state. A very high correlation between the amplitudes of the capacitance up-steps and down-steps indicates that the vesicle remains intact with no detectable material exchange between the vesicle and plasma membrane (Lollike et al., 1998; Klyachko and Jackson, 2002). An absence of lipid transfer also implies a proteinaceous pore that blocks lipid flow.

Lipid vesicles fusing with artificial bilayers in a protein-free system have the capacity to form fusion pores that close again (Chanturiya et al., 1997). Thus, lipidic fusion pores can close or reseal by a process of bilayer fission (Fig. 1, reversal of state 5 formation). A surge of content loss has been observed at the end of a kiss-and-run event, which likely reflects evolution from an initial small pore to a larger pore, followed by closure (Alés et al., 1999). This would reflect an initial sojourn in state 3 of Fig. 1, followed by a transient excursion to state 5, followed by closure. The presumed conductance increase was too brief to observe so the expansion that allowed elevated content loss must have been a very short-lived convulsion. High flux through fusion pores is occasionally followed by return to a state of low flux, somewhat below that of an initial fusion pore. Thus, a "post-spike foot" has a smaller amplitude than the earlier pre-spike foot. The pore expands and contracts back, possibly to its initial size (Mellander et al., 2012). This could reflect a state 3 → state 5 → state 3 sequence (Fig. 1). These results suggest that the transition from an initial small proteinaceous pore to a large lipidic pore is reversible.

Expansion. The fusion pore must expand to consummate the merger of the two membranes. However, expansion may be partial and reversible, with fusion pores expanding to some degree and subsequently contracting. With reference to the hypothetical structures of Fig. 1, expansion could occur during the transition from a proteinaceous pore to a lipidic pore (state 3 → state 5) or after the lipidic pore has formed (state 5 → state 6). Lipidic fusion pores are metastable and have an energy minimum defined by the elastic properties of the lipid bilayer, so expansion will be slow without some form of driving force (Chernomordik and Kozlov, 2003; Cohen and Melikyan, 2004).

Conductance measurements have shown that the abrupt initial increase representing pore opening is

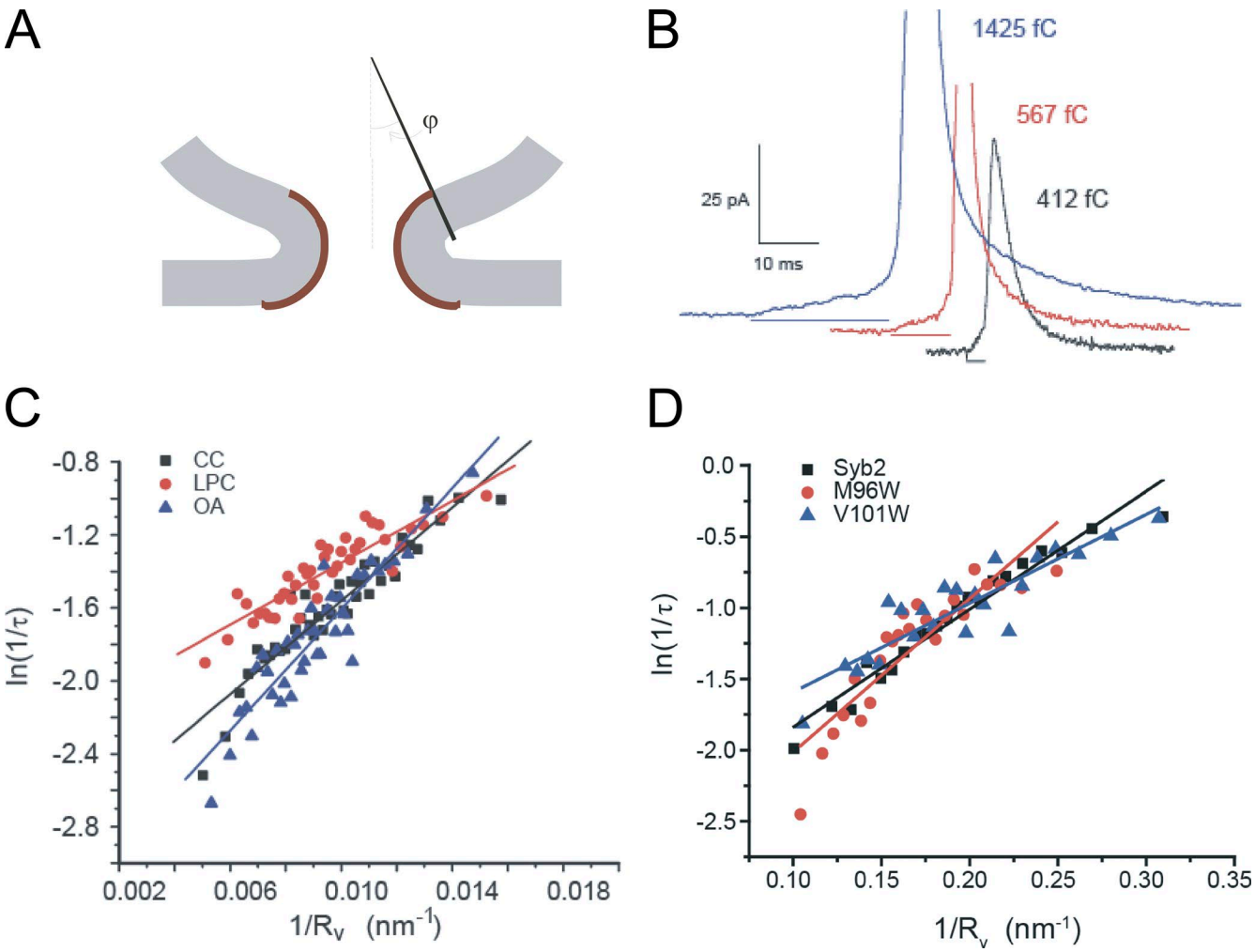

Figure 5. **Ease of formation of a lipidic fusion pore increases with decreasing vesicle size.** (A) Smaller vesicles have a larger contact angle, φ, which corresponds to a smaller area of highly curved lipid bilayer (brown). (B) Amperometry traces illustrate that larger vesicles, which contain more catecholamine, have longer duration pre-spike feet (horizontal line segments below the corresponding traces). The integrated amperometric charge in fC quantifies vesicle size. A theoretical model based on A predicts that the logarithm of the inverse pre-spike foot lifetime, τ, is a linear function of the inverse vesicle radius, R_v (proportional to the cube root of the vesicle content), and that the slope depends on the spontaneous curvature of the lipid bilayer (Zhang and Jackson, 2010). (C) Plots from rat chromaffin cells confirm this prediction and show that altering spontaneous curvature with lysophosphatidylcholine (LPC) or oleic acid (OA) changes the slope. (D) Plots from mouse chromaffin cells show that tryptophan mutations in the synaptobrevin TMD alter the slope of these plots (Chang and Jackson, 2015). The effects of both lipids (C) and mutants (D) can be interpreted in terms of changes in spontaneous curvature of the lipid bilayer.

often followed by a slower smooth increase representing graded rather than stepwise expansion (Breckenridge and Almers, 1987; Spruce et al., 1990). Fusion pore expansion can also be seen in studies with fluorescent tracers where larger tracer molecules enter vesicles at later times than smaller tracer molecules (Takahashi et al., 2002). As a pore grows, it appears to reach a point of no return beyond which closure can no longer occur (Lollike et al., 1998). This may reflect a mechanical property of lipidic fusion pores, which may only be metastable when they are small. Smaller pores can close, but reversal becomes more difficult as the pore expands.

Amperometry recordings also show the expansion of fusion pores, but the results are somewhat different from the conductance results just summarized. Amperometric pre-spike feet generally terminate abruptly with the onset of a spike, and the speed of the spike's upstroke is taken as an indication that expansion is sudden and rapid. The resolution of pre-spike feet to spikes suggests a transition from a small relatively stable pore to a large and possibly expanding pore. This transition has a steep temperature dependence, which may mean that it entails protein conformational changes (Zhang and Jackson, 2008). However, even before this transition the amplitudes of pre-spike feet sometimes grow slowly, so there may be some slow expansion before the rapid phase at the spike onset (Tang et al., 2007; Borisovska et al., 2012). The status of this slow expansion is

not clear because it is only seen in a small subpopulation of events. The expanding feet thus might be selected events from a population with no average upward drift. Overall, the amplitudes of pre-spike feet are not correlated with their duration (Wang et al., 2006), and this absence of a correlation argues against a slow expansion before the spike onset. This is an important point because it is difficult to envision how a proteinaceous pore could grow in a graded fashion.

The shapes of amperometric spikes are altered by many manipulations, including mutations or overexpression of MUNC18 (Fisher et al., 2001; Barclay, 2008), Cdk5 (Barclay et al., 2004), and CSP (Graham and Burgoyne, 2000). These actions likely reflect some effect on a later expansion of a lipidic pore. However, the weak temperature dependence of the spike rise time and decay time suggest that spike shape is determined largely by diffusion to the amperometry recording electrode (Zhang and Jackson, 2008). In fact, catecholamine diffusion has a major impact on the faster aspects of amperometric spike dynamics (Wightman et al., 1995; Haller et al., 1998), and this greatly complicates the interpretation of spike shape in terms of fusion pores.

Cytosolic Ca^{2+} accelerates fusion pore expansion (Fernández-Chacón and Alvarez de Toledo, 1995; Hartmann and Lindau, 1995; Elhamdani et al., 2006; Fulop and Smith, 2006). Amperometry recording has shown that Ca^{2+} accelerates the transition from pre-spike foot to spike, probably through Ca^{2+} binding to synaptotagmin (Wang et al., 2006). Strengthening the Ca^{2+}-dependent interaction between synaptotagmin and phosphatidylserine delays this transition (Zhang et al., 2009), whereas the expression of different synaptotagmin mutants (Bai et al., 2004; Lynch et al., 2008) and isoforms (Wang et al., 2001; Zhang et al., 2010a) can either accelerate or delay the transition. Weakening the interaction between syntaxin and polar lipids delays the transition (Lam et al., 2008). Ca^{2+}-synaptotagmin also promotes expansion of fusion pores in liposomes (Lai et al., 2013). Fusion pore expansion is accelerated by phorbol esters (Scepek et al., 1998), myosin II (Neco et al., 2008), the GTPase dynamin (Fulop et al., 2008; Anantharam et al., 2011; González-Jamett et al., 2013; Trouillon and Ewing, 2013), and another GTPase, Cdc42 (Bretou et al., 2014). Ca^{2+} regulates dynamin-mediated expansion through a signaling cascade initiated with dephosphorylation by calcineurin and mediated by interactions with syndapin and N-WASP (Samasilp et al., 2012). The content of a vesicle can influence the transition from pre-spike foot to spike, which was delayed ∼2.5-fold in vesicles containing tissue plasminogen activator-GFP versus neuropeptide Y-GFP (Weiss et al., 2014). This may reflect interactions between the vesicle matrix and membrane.

In summary, fusion pore expansion probably proceeds in two distinct phases. If the initial pore is proteinaceous, the first step could be a transformation from protein to lipid (Fig. 1, state 3 → state 5). This form of expansion requires a process by which lipid infiltrates the pore and replaces the protein (Almers, 1990). One way to achieve this is through the zipping together of the SNARE TMDs. The merger of the SNARE motif α-helix and TMD would release energy to force adjacent TMDs apart and create space for lipid to enter (discussed below; Fig. 7; Jackson, 2010). The second phase of expansion would then be a widening of the lipidic pore formed in the first phase (Fig. 1, state 5 → state 6). Because lipidic fusion pores are metastable, this will require mechanical work (Chernomordik and Kozlov, 2003; Cohen and Melikyan, 2004) or membrane tension (Kozlov and Chernomordik, 2015), and it is likely that the mechanical activity of proteins such as dynamin and myosin II is harnessed in some way. Each of these two transitions can be regulated by the fusion apparatus, and lipid bilayer elasticity plays a major role in both.

Noise. Pore conductance and content flux often display noise that is well above the instrumentation noise and thus attributable to dynamic fluctuations in fusion pore structure. Amperometry recordings from chromaffin cells display brief transient increases in flux, and these flickers were interpreted as increases in fusion pore size that could represent abortive starts toward expansion (Zhou et al., 1996). Similar brief transient enlargements of fusion pores were also reported for dopamine release from neurons (Staal et al., 2004). Experiments with synaptobrevin mutants support the interpretation of flickers as abortive expansions. Lengthening the linker between the SNARE motif and TMD eliminated the flickers, presumably by weakening the ability of SNAREs to transmit force to the membrane (Kesavan et al., 2007). When mutations weakened interactions between SNARE TMDs, the initial fusion pores spent more time in an initial state with more frequent flickers suggestive of repeated unsuccessful attempts to expand (Wu et al., 2016).

The conductance is very noisy in fusion pores formed by protein-free lipid vesicles and bilayers (Chanturiya et al., 1997). Similarly, large fluctuations in conductance appear in dense-core vesicle fusion pores when they become large (Monck et al., 1990; Spruce et al., 1990; Curran et al., 1993). This parallel is intriguing and may reflect similarities in composition. These fluctuations in large pores are quite slow and different from the rapid flickers described in the preceding paragraph. The rapid flickers may be a characteristic of early-stage small proteinaceous pores, whereas the slower fluctuations of large pores may be a characteristic of late-stage large lipidic pores.

Energies of hypothesized structures

Models generally posit specific molecular interactions for which energies can be estimated. Very high energies imply that a structure will be difficult to form and this provides a basis for evaluating the plausibility of a model. In general, the state of our understanding of molecular forces does not permit quantitative calculations of energies, especially in the absence of a detailed structure. Nevertheless, qualitative estimates have helped guide the field in considering various models.

Membrane elasticity. Lipid bilayers have elastic properties that define the energetics of a variety of deformations, including out of plane bending (Helfrich, 1973). The initial contact (Fig. 1, state 2) and proteinaceous pore (Fig. 1, state 3) can form with minimal bending of the lipid bilayers, but formation of a lipidic fusion pore requires bending a bilayer to the point where its radius of curvature is almost as small as the membrane thickness. Thus, there is a large energy barrier to the formation of a lipidic fusion pore. This energy can be analyzed mathematically and expressed in terms of the fusion pore's shape and the elastic moduli of a lipid bilayer. The curvature at any position on the membrane is written as a sum of two terms, referred to as the mean curvature and Gaussian (or splay) curvature. The total Gaussian curvature of a surface does not depend on the details of the shape but only topology. Regardless of the shape, the Gaussian curvature of two separate closed membranes differs from that of a single closed membrane by -4π (Kreyszig, 1991; Siegel, 2008). However, estimating the change in energy is difficult because the Gaussian curvature modulus is very difficult to measure. The Gaussian curvature may contribute as much as 100 kT to the energy of forming a fusion pore from two separate membranes (Siegel, 2008). In contrast, the elastic modulus for mean curvature is well known (Marsh, 2006), so this contribution to the fusion pore bending energy can be estimated by integrating the mean curvature over a hypothesized surface.

Early efforts to calculate the mean curvature assumed that a lipid fusion pore has a toroidal shape (Kozlov et al., 1989; Chizmadzhev et al., 1995), and this led to very high energies. However, the assumption of toroidal geometry overestimates the mean curvature. A toroid can deform to a surface that qualitatively resembles a catenoid (a surface of revolution formed by a hyperbolic cosine function), and this shape has zero mean curvature at every point (Kreyszig, 1991). The actual energy of a fusion pore falls between these two extremes, and to determine this energy requires finding the shape that minimizes the mean curvature (and thus minimizes the pore energy). When this is done (with a simultaneous minimization for both monolayers of the bilayer), it can be seen that a fusion pore can assume shapes that have a significant bending energy well below the value obtained for a toroid (Jackson, 2009). Further variations of shape that incorporated additional detail showed that a fusion pore can assume a "bowing" or "teardrop" shape. This additional reduction in mean curvature energy required that the pore extend laterally over distances of more than 10 times the pore radius (Ryham et al., 2013; Yoo et al., 2013). A very different approach to this problem uses an intermediate level of detail to treat the intermolecular forces between lipids. By avoiding continuum mechanics, this approach gets around the problem of not knowing the Gaussian curvature modulus. This approach yielded fairly low energies, in the range of 10–20 kT (Katsov et al., 2004).

Although the mathematical analysis leaves the actual value of the energy of formation of a lipidic fusion pore unclear, these efforts have produced the important result that a fusion pore formed by bending a lipid bilayer is metastable; it has a minimum energy at a particular radius and bilayer separation (Katsov et al., 2004; Jackson, 2009). Fig. 6 illustrates this feature for the continuum elasticity model. Structures such as the one illustrated in Fig. 6 A have a minimum amount of mean curvature. Fixing the bilayer separation distance (R_b) and varying the pore radius (R_p) gives minima with much lower energies for lipids with negative spontaneous curvature (Fig. 6 B). Allowing both R_p and R_b to vary locates a global energy minimum (Fig. 6 C). This means that once it forms, a lipidic fusion pore can linger in a narrow hourglass shape without expanding or resealing. Perhaps thermal fluctuations can drive transitions out of this minimum, but cellular machinery can accelerate these processes. A role for mechanical work by proteins was discussed above in connection with fusion pore expansion. The important point is that fusion is not complete when the lipidic fusion pore forms, even though the vesicle and plasma membrane bilayers have merged and become contiguous. Fusion pores face an energy barrier for expansion (Chernomordik and Kozlov, 2003; Cohen and Melikyan, 2004), and force generating proteins or membrane tension (Kozlov and Chernomordik, 2015) are needed to drive the process to completion.

Hydrophobic interfacial energy. Membrane fusion entails substantial remodeling of lipid bilayers, and hypothetical fusion mechanisms can include intermediates with varying amounts of exposure between water and the hydrophobic interior of the lipid bilayer. A simple way to estimate this energy is to calculate the surface area of this contact and multiply by a parameter based on experiments with model compounds. However, the choice for this parameter led to some confusion. Interfacial tension measurements yield a value of roughly 72 cal/Å^2 (50 erg/cm^2), whereas solvent partitioning measurements yield a value of roughly 25 cal/Å^2 (Tanford,

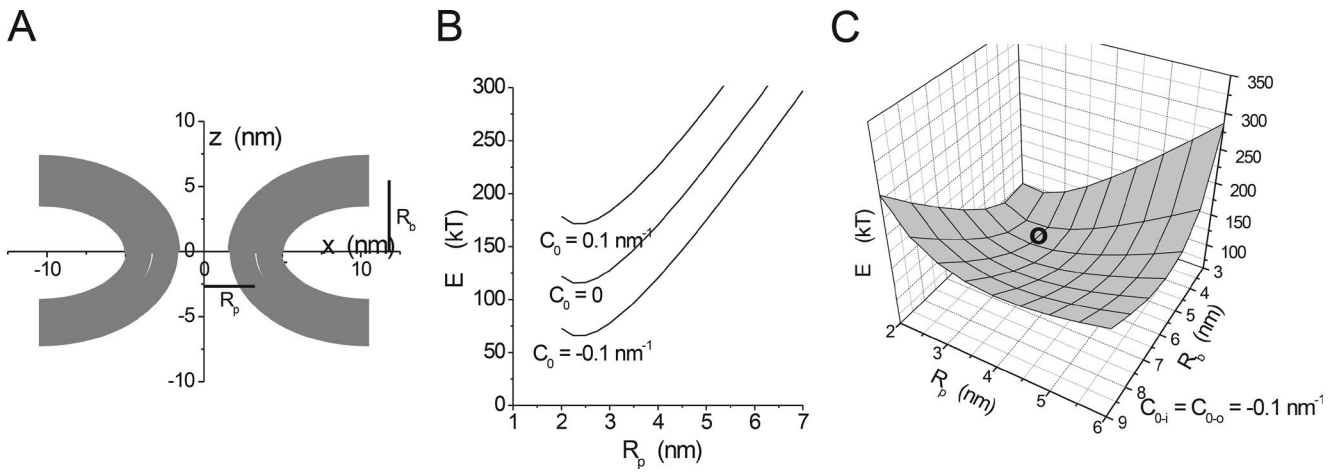

Figure 6. **Minimum energy fusion pores.** (A) The fusion pore is a surface of revolution around the z axis formed by a lipid bilayer. This shape was obtained by minimizing the mean curvature of two parallel lipid monolayers subject to the constraint of a pore radius R_p = 3.3 nm and a bilayer separation of twice R_b = 5.45 nm (note that these are distances to the center of the bilayer; further note that this minimization omitted the possibility of an inflection that can introduce a bowing shape that reduces the energy further; Yoo et al., 2013). (B) Minimum energies determined for R_b = 3 nm and varied R_p. This plot shows a stable minimum at R_p = ∼2.5 nm. The spontaneous curvature of the lipid (C_0) has a major influence on the energy but not on the position of the minimum. (C) Varying both R_p and R_b reveals a global minimum at the location indicated by the circle, at R_p = 2.75 nm and R_b = 4.2 nm (modified from Jackson [2009] with permission from Springer).

1979). This discrepancy arises from the restriction of hydrocarbon rotations at the aqueous interface (Jackson, 2016), but this factor is irrelevant to interactions during membrane fusion. Thus, Tanford's solvent partitioning parameter of ∼25 cal/Å^2 is what should be used, and in a model for fusion pore expansion in which the lipid hydrocarbon chains become exposed to water, the energy of the resulting barrier allows for expansion on a millisecond timescale (Jackson, 2010).

Hydration repulsive force. Bringing two lipid bilayers together requires dehydration of the polar head groups (Rand, 1981). This gives rise to a steeply rising repulsive force between two lipid bilayers and the initiation of fusion must overcome this force.

Transitions. Energetic considerations offer a perspective on the different hypothetical structures summarized in Fig. 1. The various transitions between putative structures entail different degrees of changes in membrane bending, hydrocarbon–water contact, and lipid head group distances.

Transition 1 → 2: This transition precedes fusion pore formation. It entails associations between proteins in the two membranes, presumably SNAREs, as they undergo an early stage of zipping. It probably entails some deformation of the two membranes around the proteins pulling them together. The protein–protein association then works against the membrane bending and hydration repulsion to create a dimple that reflects the balance between these three forces.

Transition 2 → 3: The proteins holding the two membranes together can form a nascent fusion pore, presumably with SNARE TMDs (Fig. 4). A connection with associated proteins (Fig. 1, state 2b) could act as a closed channel. During this transition, there should be little work done on the elastic or repulsive forces of the lipid bilayers.

Transition 2 → 5: This alternative route for pore formation has not been explicitly proposed, but if there are too few SNAREs to form a channel and the C termini of SNARE TMDs are pulled into the membrane (Ngatchou et al., 2010; Lindau et al., 2012), the result could be a direct transition to a lipidic pore. This transition would thus bypass the lipid stalk (Fig. 1, state 4a) and hemifusion diaphragm (Fig. 1, state 4b). The mechanism proposed for fusion pore expansion by helix completion in SNAREs (Jackson, 2010) could drive this transition, but with fewer SNAREs than are needed to form a proteinaceous channel.

Transition 2 → 4: The formation of a hemifusion diaphragm is widely accepted as an intermediate in lipid bilayer fusion in the absence of protein as well as in viral fusion. Electron tomography images revealed large numbers of synaptic vesicles hemifused with the plasma membrane in the active zone in the absence of fusion (Zampighi et al., 2006), but another study reported that direct vesicle membrane contact with the plasma membrane depended on stimulation to elicit membrane fusion (Fernández-Busnadiego et al., 2010). The observation of membrane flux before pore opening supports the existence of a hemifused structure (Zhao et al., 2016). Connection by separate proteins (Fig. 1, state 2a) is a more likely precursor for a stalk (Fig. 1, state 4a) because this could force the bilayers surrounded by the contacts together. The merger of

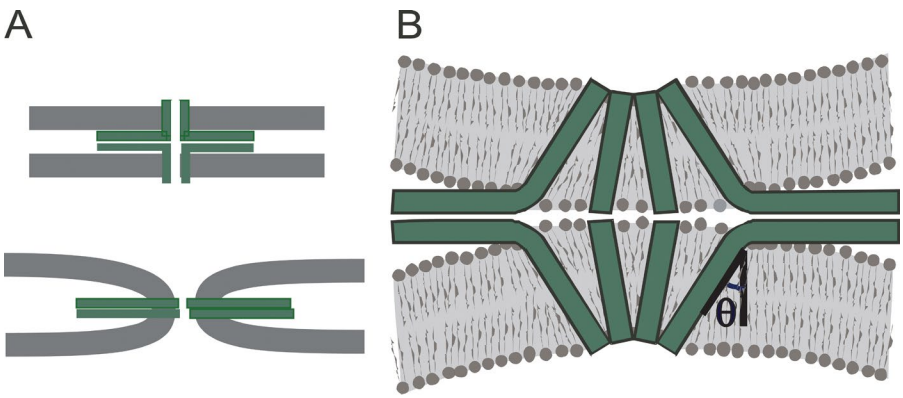

Figure 7. **A model for transition 3 → 5.** (A) The joining of the helical segments of the SNARE motif with the helical TMD is a potential driving force for this transition. In the initial state (top), the SNARE motifs are perpendicular to the TMDs (high energy) and the membranes are flat (low energy). The final state (bottom) has straight SNAREs (low energy) and curved membrane (high energy). (B) As the transition progresses, the hydrocarbon interior becomes transiently exposed to water, creating a barrier to the transition. The angle θ between the TMD and the membrane normal serves as a reaction coordinate for the transition (Jackson, 2010).

the proximal monolayers has a substantial cost in lipid bending associated with Gaussian curvature, and the distal monolayers must be highly curved at the rim, so reaching this state will be energetically costly. Forming a stalk or hemifusion diaphragm has the advantage of distributing the large change in Gaussian curvature energy between two steps.

Transition 3 → 5: The transition from a proteinaceous pore to a lipidic pore presumably involves some degree of expansion. This transition was hypothesized early in studies of fusion pores (Almers, 1990), but how it occurs remains a subject of speculation. It faces a large barrier from bilayer bending (Zhang and Jackson, 2010; Chang and Jackson, 2015). The driving force provided by SNARE complex zipping and the joining of the α-helices of the SNARE motifs and TMDs may be sufficient to overcome this barrier (Fig. 7 A), as well as a barrier resulting from the transient exposure of lipid hydrocarbon chains to water (Fig. 7 B; Jackson, 2010).

Transition 4 → 5: Expansion and monolayer bending at the rim of the hemifusion diaphragm both will impose tension on the bilayer to drive the formation of a channel through the bilayer formed by the two distal monolayers (Kozlov et al., 1989; Chernomordik and Kozlov, 2003; Ryham et al., 2016). A lipid-lined pore through the bilayer of the hemifusion diaphragm would then expand to a lipidic fusion pore. So this transition proceeds in the stages (1) stalk expansion to a diaphragm (4a → 4b), (2) pore formation through the diaphragm, (3) transbilayer pore expansion to the lipidic pore.

Transition 5 → 6: Membrane elasticity resists the growth of lipidic fusion pores. This transition is probably driven by motor proteins and membrane tension as discussed above (Dynamic properties–Expansion).

Synaptic release and fusion pores

Synaptic transmission depends on exocytosis, but synaptic fusion pores are difficult to study. The relation between fusion pore flux and synaptic response is not clear. There is quite a bit of speculation about the roles of fusion pores in synaptic function and plasticity but only a few examples where manipulations of exocytosis proteins influence the shape of a synaptic current (Pawlu et al., 2004; Guzman et al., 2010). However, kiss-and-run at synapses produces much lower concentrations of neurotransmitter in the synaptic cleft (Richards, 2009).

Synaptic transmission proceeds through a sequence of steps: Ca^{2+} entry, Ca^{2+} binding, structural transitions in the fusion apparatus, fusion pore opening/expansion, neurotransmitter flux through the fusion pore, neurotransmitter diffusion across the synaptic cleft, and postsynaptic receptor activation. Synaptic delays are on the order of a hundred microseconds and reflect the sum of the times for all these steps. Neurotransmitter expulsion must be briefer than this aggregate time to minimize its contribution to the delay. By this reasoning, the expulsion step should be less than ∼100 µs.

The relationship between flux and conductance discussed above (Transport properties–Content flux and conductance) permits an analysis of the impact of pore size on the speed of synaptic release. If a vesicle loses content with a rate proportional to the intravesicular concentration, then as molecules flow through a stable fusion pore, the number of molecules in the vesicle, N, decays exponentially with time.

$$N = N_0 e^{-\alpha t}. \quad (2)$$

With knowledge of the number of transmitter molecules in a vesicle and the flux through a fusion pore, we can estimate α and obtain the expulsion time τ as $1/\alpha$. The initial rate of transmitter expulsion will be the derivative of Eq. 2 at $t = 0$ or αN_0. With N_0 = 1,600 molecules of glutamate in the synaptic vesicle of an excitatory glutamatergic synapse (Edwards, 1995) and the ratio of flux to conductance cited above (Gong et al., 2007), we obtain $\alpha 1600 = 2.2 \times 10^7$ molecules s^{-1} nS^{-1}, from which we can take $1/\alpha$ as

$$\tau = 73\ \gamma^{-1}\ \mu s, \quad (3)$$

where γ is the fusion pore conductance in nanosiemens. By this reasoning, a 1-nS fusion pore will allow a vesicle to expel its content in a sufficiently brief time of 73 μs. However, 1 nS is extremely large; measurements of fusion pores for synaptic (He et al., 2006) and synaptic-like (Klyachko and Jackson, 2002) vesicles are <100 pS. This would lead to an expulsion time of >730 μs, which is longer than typical synaptic delays at rapid synapses. It should be noted that this calculation used fusion pore flux measurements for catecholamines; epinephrine and norepinephrine have molecular masses of 183 D and 169 D, respectively. Glutamate and acetylcholine have molecular masses of 147 D and 146 D, respectively. These somewhat smaller molecules should pass through a fusion pore a bit more rapidly (Braun et al., 2007), but this difference will not have a major impact, so the result for catecholamine should be applicable to excitatory synapses. Eq. 3 is an improvement over previous efforts to address this issue in that it does not depend on assumptions of pore geometry; we did not require an estimate of its radius. By using the flux to conductance ratio (Gong et al., 2007) and experimental measurements of the conductance of relevant fusion pores, we can estimate the speed of transmitter expulsion. The result clearly indicates that the conductance of initial pores formed by fusing synaptic vesicles would not allow transmitter expulsion with sufficient speed and would increase the synaptic delay above that observed.

The interplay between the rate of release and the rate of diffusion radially away from the site of release provides another basis for assessing the need for speed. The synaptic cleft provides space for diffusion, and after passing through the fusion pore, diffusion within the synaptic cleft will dilute the transmitter. This may prevent the local concentration from getting high enough to activate postsynaptic receptors. To activate receptors, neurotransmitter must come out faster than this radial diffusion. This problem has been studied with simple diffusion models (Khanin et al., 1994) as well as sophisticated computer models (Clements, 1996; Stiles et al., 1996; Wahl et al., 1996). The sophisticated models are generally overkill because the underlying process is simple. Flux through the fusion pore will increase the number of transmitter molecules in the cleft according to Eq. 2. At a given time *s*, the total number of released molecules will increase by $N_0\alpha e^{-\alpha s}ds$. This addition of molecules to the cleft will initially have a sharply peaked distribution (a delta function) and will spread out so that at a later time *t* the distribution will be described by the solution to the diffusion equation in two dimensions:

$$N_s(z,t) = \frac{N_0\alpha\, e^{-\alpha s}\,ds}{4\pi D(t-s)}\, e^{-z^2/4D(t-s)}, \quad (4)$$

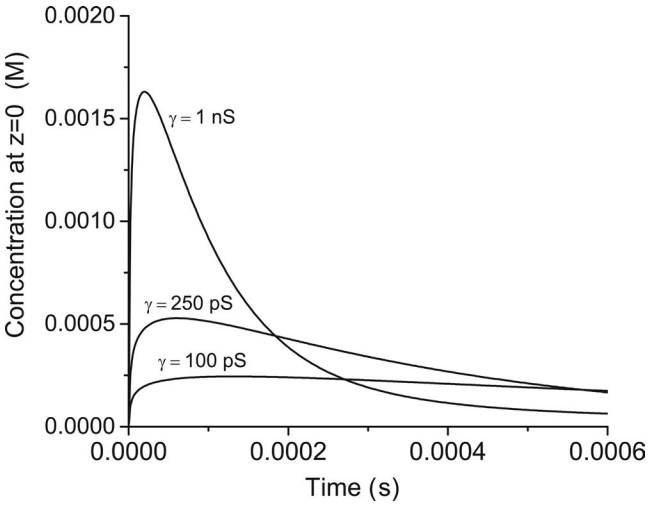

Figure 8. **The time course of concentration within the synaptic cleft.** The concentration directly under the release site was obtained by integrating Eq. 5 at $z = 0$. α was calculated from Eq. 2 for the indicated values of conductance. N_0 = 1,600 (Edwards, 1995) and D = 0.33 μm^2 ms^{-1} (Nielsen et al., 2004). To convert to *N* to concentration a thickness of the synaptic cleft was taken as 20 nm.

where *z* is the radial distance within the cleft from the release site. Integrating over these increments from the time of fusion pore opening, $s = 0$, to a later time, $s = t$ (convoluting Eq. 4 with the exponentially decaying release rate), then gives the time course of molecule number as a function of position and time:

$$N(z,t) = \frac{N_0\alpha}{4\pi D}\int_0^t \frac{e^{-\alpha s}e^{-z^2/4D(t-s)}}{t-s}\,ds. \quad (5)$$

Eq. 5 was integrated numerically at $z = 0$ (directly under the release site) and $N(z, t)$ converted to concentration. The calculation incorporated a measured diffusion constant of glutamate in the synaptic cleft of a cerebellar excitatory synapse of 0.33 μm^2/ms (Nielsen et al., 2004), N_0 as 1600 (Edwards, 1995), and $\alpha = 1/\tau$ from Eq. 3. Fig. 8 plots the results for a few different values of fusion pore conductance. With a fusion pore conductance of 1 nS, transmitter concentration rapidly rises to levels >1 mM, which is sufficient to activate AMPA-type glutamate receptors (Clements, 1996). However, as already noted, 1 nS is over an order of magnitude larger than fusion pores associated with synaptic vesicles. With smaller values of γ, the subsynaptic concentration cannot rise to levels high enough to activate glutamate receptors to the degree that must occur. This analysis confirms prior work but without assumptions of the geometry or structure of the fusion pore.

This analysis strengthens the aforementioned conclusion that the initial fusion pores formed by vesicles during fusion are much too small to support rapid synaptic transmission. Synaptic release depends on forma-

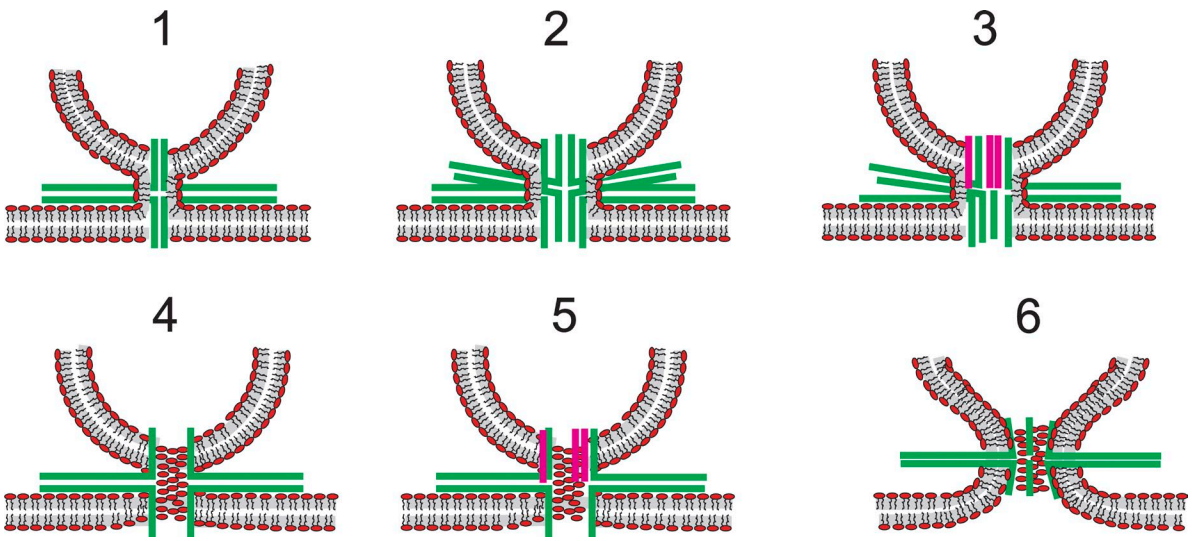

Figure 9. **Composite lipid–protein fusion pores.** SNAREs are green; synaptophysin TMDs are pink. Models 1–3 illustrate continuity of the proximal monolayer of the vesicle and plasma membrane outside a proteinaceous fusion pore. These models have no contact between phospholipids and the aqueous pore lumen. Models 4–5 illustrate lipid headgroups of a bilayer that forms a pore in which lipid and protein alternate along the walls. Model 6 illustrates protein TMDs lodged among the headgroups of a lipidic fusion pore.

tion of a later stage in the evolution of the fusion pore. Some expansion must occur. Kiss-and-run release is still possible, but closure must occur after the pore has expanded to a size corresponding to a conductance in the order of 1 nS.

Conclusions and future directions

A large body of work using several different experimental techniques has demonstrated that fusion pores are dynamic and can assume multiple functionally distinct states. During Ca^{2+}-triggered exocytosis, cells can regulate which of these states form, how long they last, whether they grow or shrink, and whether they resolve to full membrane merger or reverse and reseal. Several studies have shown that fusion pores can filter molecules of different sizes and that pore selectivity can be shaped by the conditions used to elicit secretion. The next challenge is connecting this selectivity to the putative structures for fusion pores. We will need a better understanding of these structures to assign functions to the molecules of the fusion apparatus.

The nature of the initial fusion pore is critical to the mechanism of exocytosis. Whether the initial fusion pore is lipid or protein defines the underlying process as one in which lipids are the primary actors and engage with the assistance of proteins, or proteins are the primary actors, taking the initiative and forcing the lipids to follow. This relates to the broader poorly understood questions of physical mechanisms by which proteins shape and remodel membranes.

A general trend that has emerged from the work on fusion pores is that smaller fusion pores tend to have properties more closely aligned with a protein composition, whereas larger fusion pores behave as expected for curved lipid bilayers. The lipidic pore (Fig. 1, state 5) can account for virtually all of the observations of large fusion pores formed after an initial delay, but with small pores neither the purely proteinaceous structure (Fig. 1, state 3) nor purely lipidic structure accounts for all of the experimental results. The proteinaceous model is consistent with the effects of TMD mutations (Han et al., 2004; Han and Jackson, 2005; Chang et al., 2015; Bao et al., 2016), structural work on the synaptobrevin–synaptophysin complex (Adams et al., 2015), low conductance (Klyachko and Jackson, 2002; He et al., 2006; Jackson, 2009), ease of reversal (Henkel et al., 2000), and low initial membrane bending strain (Zhang and Jackson, 2010; Chang and Jackson, 2015). However, the small number of SNAREs required for fusion (Mohrmann et al., 2010; van den Bogaart et al., 2010; Sinha et al., 2011; Bao et al., 2016) indicates that the pore must contain other proteins (non-SNAREs) or lipid, and the observation of lipid flux before aqueous pore opening (Zhao et al., 2016) indicates the pore must contain lipids. To reconcile the large bodies of data that point to both types of initial fusion pore, it may be necessary to consider a new class of models that are neither entirely protein nor entirely lipid. Fusion pores may be composite or hybrid, with a structure not pictured in Fig. 1.

The idea of a composite protein–lipid fusion pore has been proposed on several occasions (Zimmerberg et al., 1991; Jackson and Chapman, 2006; Jackson, 2007; Fang et al., 2008; Bao et al., 2016), but discussions of explicit structures have been limited. The problem is that it is difficult to come up with plausible models.

Fig. 9 presents a few ideas for fusion pores composed of protein and lipid, including some with synaptophysin. One might hypothesize that a lipid monolayer forms a continuous lining around a proteinaceous channel that is either closed (Fig. 9, model 1) or open (Fig. 9, model 2). This monolayer connects the cytoplasmic leaflets of the vesicle and plasma membrane and would allow both lipid transport and contact of TMD residues with the aqueous pore lumen. This idea can readily be extended to include synaptophysin (Fig. 9, model 3). This model requires an extreme amount curvature in the fused proximal monolayer and also requires a large number of TMDs to fully encompass the pore. These models can account for early lipid transfer, but if the pore is entirely surrounded by SNARE TMDs, the number of SNAREs would exceed experimental estimates. Incorporating synaptophysin would reduce the number of synaptobrevin TMDs, possibly reconciling the need for only two copies (Sinha et al., 2011). Furthermore, although several TMDs of syntaxin would still be required, if they are paired with fewer synaptobrevins, some of the unpaired syntaxin SNARE motifs could be incorporated into heterodimers with SNAP-25 (Fasshauer and Margittai, 2004), possibly reconciling the need for only three copies of SNAP-25 (Mohrmann et al., 2010). One might also hypothesize that both TMDs and lipids surround the aqueous lumen (Fig. 9, models 4–6). In such structures, the TMDs would interact with the aqueous lumen, but fewer TMDs would be needed. Such fusion pores would require extreme membrane curvature, but the amount of lipid bilayer strained in this way would be lower than in a purely lipidic pore of the same size. In such a pore, the TMDs could serve as a boundary, with hydrocarbon chains on one side and polar head groups on the other (Fig. 9, models 4–5). Alternatively, the TMDs could be lodged near the headgroups, as has been seen in protein–lipid pores through bilayers formed by a Bax-derived peptide (Qian et al., 2008). But this would require pulling some of the SNARE motif and linker into the bilayer and taking a shorter segment of the TMD as pore liner (Fig. 9, model 6).

The structures put forward in Fig. 9 all have problems, and their plausibility may not hold up to critical examination, but it is important for investigators to start thinking more explicitly about composite lipid–protein fusion pores. Furthermore, these models can be tested. They make different predictions about the time of establishing a lipid connection between the distal and proximal monolayers. So far, only the proximal monolayer has been examined in cellular exocytosis (Zhao et al., 2016). These models could also be tested by estimating minimal numbers for all three synaptic SNAREs, as well as synaptophysin, in the same cellular system. Finally, it will be worthwhile to test the role of synaptophysin TMDs in fusion pores.

It is quite possible that there are fusion intermediates that have yet to be imagined, and thoughtful modeling of lipid–protein interactions may provide new ideas for experimental testing. Further work and improvements in techniques for studying fusion pores are certain to open up new possibilities and improve our understanding of the structure and composition of different fusion intermediates. By understanding the nature of these states and how cells control the progression, we will realize the goal of having a detailed mechanism of membrane fusion. This will in turn enhance our understanding of important biological processes in the regulation of chemical signaling.

ACKNOWLEDGMENTS

We thank Ed Chapman and Sam Condon for comments on the manuscript.

This work was funded by National Institutes of Health grant NS44057.

The authors declare no competing financial interests.

Lesley C. Anson served as editor.

Submitted: 5 November 2016
Accepted: 19 January 2017

REFERENCES

Adams, D.J., C.P. Arthur, and M.H. Stowell. 2015. Architecture of the synaptophysin/synaptobrevin complex: Structural evidence for an entropic clustering function at the synapse. *Sci. Rep.* 5:13659. http://dx.doi.org/10.1038/srep13659

Albillos, A., G. Dernick, H. Horstmann, W. Almers, G. Alvarez de Toledo, and M. Lindau. 1997. The exocytotic event in chromaffin cells revealed by patch amperometry. *Nature.* 389:509–512. http://dx.doi.org/10.1038/39081

Alés, E., L. Tabares, J.M. Poyato, V. Valero, M. Lindau, and G. Alvarez de Toledo. 1999. High calcium concentrations shift the mode of exocytosis to the kiss-and-run mechanism. *Nat. Cell Biol.* 1:40–44.

Almers, W. 1990. Exocytosis. *Annu. Rev. Physiol.* 52:607–624. http://dx.doi.org/10.1146/annurev.ph.52.030190.003135

Alvarez de Toledo, G., R. Fernández-Chacón, and J.M. Fernández. 1993. Release of secretory products during transient vesicle fusion. *Nature.* 363:554–558. http://dx.doi.org/10.1038/363554a0

Anantharam, A., M.A. Bittner, R.L. Aikman, E.L. Stuenkel, S.L. Schmid, D. Axelrod, and R.W. Holz. 2011. A new role for the dynamin GTPase in the regulation of fusion pore expansion. *Mol. Biol. Cell.* 22:1907–1918. http://dx.doi.org/10.1091/mbc.E11-02-0101

Aravanis, A.M., J.L. Pyle, and R.W. Tsien. 2003. Single synaptic vesicles fusing transiently and successively without loss of identity. *Nature.* 423:643–647. http://dx.doi.org/10.1038/nature01686

Arthur, C.P., and M.H. Stowell. 2007. Structure of synaptophysin: a hexameric MARVEL-domain channel protein. *Structure.* 15:707–714. http://dx.doi.org/10.1016/j.str.2007.04.011

Bai, J., C.T. Wang, D.A. Richards, M.B. Jackson, and E.R. Chapman. 2004. Fusion pore dynamics are regulated by synaptotagmin*t-SNARE interactions. *Neuron.* 41:929–942. http://dx.doi.org/10.1016/S0896-6273(04)00117-5

Bao, H., M. Goldschen-Ohm, P. Jeggle, B. Chanda, J.M. Edwardson, and E.R. Chapman. 2016. Exocytotic fusion pores are composed of both lipids and proteins. *Nat. Struct. Mol. Biol.* 23:67–73. http://dx.doi.org/10.1038/nsmb.3141

Barclay, J.W. 2008. Munc-18-1 regulates the initial release rate of exocytosis. *Biophys. J.* 94:1084–1093. http://dx.doi.org/10.1529/biophysj.107.111203

Barclay, J.W., M. Aldea, T.J. Craig, A. Morgan, and R.D. Burgoyne. 2004. Regulation of the fusion pore conductance during exocytosis by cyclin-dependent kinase 5. *J. Biol. Chem.* 279:41495–41503. http://dx.doi.org/10.1074/jbc.M406670200

Barg, S., C.S. Olofsson, J. Schriever-Abeln, A. Wendt, S. Gebre-Medhin, E. Renström, and P. Rorsman. 2002. Delay between fusion pore opening and peptide release from large dense-core vesicles in neuroendocrine cells. *Neuron.* 33:287–299. http://dx.doi.org/10.1016/S0896-6273(02)00563-9

Borisovska, M., Y.N. Schwarz, M. Dhara, A. Yarzagaray, S. Hugo, D. Narzi, S.W. Siu, J. Kesavan, R. Mohrmann, R.A. Böckmann, and D. Bruns. 2012. Membrane-proximal tryptophans of synaptobrevin II stabilize priming of secretory vesicles. *J. Neurosci.* 32:15983–15997. http://dx.doi.org/10.1523/JNEUROSCI.6282-11.2012

Braun, M., A. Wendt, J. Karanauskaite, J. Galvanovskis, A. Clark, P.E. MacDonald, and P. Rorsman. 2007. Corelease and differential exit via the fusion pore of GABA, serotonin, and ATP from LDCV in rat pancreatic beta cells. *J. Gen. Physiol.* 129:221–231. http://dx.doi.org/10.1085/jgp.200609658

Breckenridge, L.J., and W. Almers. 1987. Currents through the fusion pore that forms during exocytosis of a secretory vesicle. *Nature.* 328:814–817. http://dx.doi.org/10.1038/328814a0

Bretou, M., O. Jouannot, I. Fanget, P. Pierobon, N. Larochette, P. Gestraud, M. Guillon, V. Emiliani, S. Gasman, C. Desnos, et al. 2014. Cdc42 controls the dilation of the exocytotic fusion pore by regulating membrane tension. *Mol. Biol. Cell.* 25:3195–3209. http://dx.doi.org/10.1091/mbc.E14-07-1229

Chandler, D.E. 1991. Membrane fusion as seen in rapidly frozen secretory cells. *Ann. N. Y. Acad. Sci.* 635:234–245. http://dx.doi.org/10.1111/j.1749-6632.1991.tb36495.x

Chang, C.W., and M.B. Jackson. 2015. Synaptobrevin transmembrane domain influences exocytosis by perturbing vesicle membrane curvature. *Biophys. J.* 109:76–84. http://dx.doi.org/10.1016/j.bpj.2015.05.021

Chang, C.W., E. Hui, J. Bai, D. Bruns, E.R. Chapman, and M.B. Jackson. 2015. A structural role for the synaptobrevin 2 transmembrane domain in dense-core vesicle fusion pores. *J. Neurosci.* 35:5772–5780. http://dx.doi.org/10.1523/JNEUROSCI.3983-14.2015

Chang, C.W., C.W. Chiang, J.D. Gaffaney, E.R. Chapman, and M.B. Jackson. 2016. Lipid-anchored synaptobrevin provides little or no support for exocytosis or liposome fusion. *J. Biol. Chem.* 291:2848–2857. http://dx.doi.org/10.1074/jbc.M115.701169

Chanturiya, A., L.V. Chernomordik, and J. Zimmerberg. 1997. Flickering fusion pores comparable with initial exocytotic pores occur in protein-free phospholipid bilayers. *Proc. Natl. Acad. Sci. USA.* 94:14423–14428. http://dx.doi.org/10.1073/pnas.94.26.14423

Chernomordik, L.V., and M.M. Kozlov. 2003. Protein-lipid interplay in fusion and fission of biological membranes. *Annu. Rev. Biochem.* 72:175–207. http://dx.doi.org/10.1146/annurev.biochem.72.121801.161504

Chizmadzhev, Y.A., F.S. Cohen, A. Shcherbakov, and J. Zimmerberg. 1995. Membrane mechanics can account for fusion pore dilation in stages. *Biophys. J.* 69:2489–2500. http://dx.doi.org/10.1016/S0006-3495(95)80119-0

Chizmadzhev, Y.A., D.A. Kumenko, P.I. Kuzmin, L.V. Chernomordik, J. Zimmerberg, and F.S. Cohen. 1999. Lipid flow through fusion pores connecting membranes of different tensions. *Biophys. J.* 76:2951–2965. http://dx.doi.org/10.1016/S0006-3495(99)77450-3

Chow, R.H., L. von Rüden, and E. Neher. 1992. Delay in vesicle fusion revealed by electrochemical monitoring of single secretory events in adrenal chromaffin cells. *Nature.* 356:60–63. http://dx.doi.org/10.1038/356060a0

Clements, J.D. 1996. Transmitter timecourse in the synaptic cleft: its role in central synaptic function. *Trends Neurosci.* 19:163–171. http://dx.doi.org/10.1016/S0166-2236(96)10024-2

Cohen, F.S., and G.B. Melikyan. 2004. The energetics of membrane fusion from binding, through hemifusion, pore formation, and pore enlargement. *J. Membr. Biol.* 199:1–14. http://dx.doi.org/10.1007/s00232-004-0669-8

Curran, M.J., F.S. Cohen, D.E. Chandler, P.J. Munson, and J. Zimmerberg. 1993. Exocytotic fusion pores exhibit semi-stable states. *J. Membr. Biol.* 133:61–75. http://dx.doi.org/10.1007/BF00231878

Dhara, M., A. Yarzagaray, M. Makke, B. Schindeldecker, Y. Schwarz, A. Shaaban, S. Sharma, R.A. Böckmann, M. Lindau, R. Mohrmann, and D. Bruns. 2016. v-SNARE transmembrane domains function as catalysts for vesicle fusion. *eLife.* 5:e17571. http://dx.doi.org/10.7554/eLife.17571

Domanska, M.K., V. Kiessling, and L.K. Tamm. 2010. Docking and fast fusion of synaptobrevin vesicles depends on the lipid compositions of the vesicle and the acceptor SNARE complex-containing target membrane. *Biophys. J.* 99:2936–2946. http://dx.doi.org/10.1016/j.bpj.2010.09.011

Edwards, F.A. 1995. Anatomy and electrophysiology of fast central synapses lead to a structural model for long-term potentiation. *Physiol. Rev.* 75:759–787.

Elhamdani, A., F. Azizi, and C.R. Artalejo. 2006. Double patch clamp reveals that transient fusion (kiss-and-run) is a major mechanism of secretion in calf adrenal chromaffin cells: high calcium shifts the mechanism from kiss-and-run to complete fusion. *J. Neurosci.* 26:3030–3036. http://dx.doi.org/10.1523/JNEUROSCI.5275-05.2006

Fang, Q., K. Berberian, L.W. Gong, I. Hafez, J.B. Sørensen, and M. Lindau. 2008. The role of the C terminus of the SNARE protein SNAP-25 in fusion pore opening and a model for fusion pore mechanics. *Proc. Natl. Acad. Sci. USA.* 105:15388–15392. http://dx.doi.org/10.1073/pnas.0805377105

Fasshauer, D., and M. Margittai. 2004. A transient N-terminal interaction of SNAP-25 and syntaxin nucleates SNARE assembly. *J. Biol. Chem.* 279:7613–7621. http://dx.doi.org/10.1074/jbc.M312064200

Fernandez, J.M., E. Neher, and B.D. Gomperts. 1984. Capacitance measurements reveal stepwise fusion events in degranulating mast cells. *Nature.* 312:453–455. http://dx.doi.org/10.1038/312453a0

Fernández-Busnadiego, R., B. Zuber, U.E. Maurer, M. Cyrklaff, W. Baumeister, and V. Lucic. 2010. Quantitative analysis of the native presynaptic cytomatrix by cryoelectron tomography. *J. Cell Biol.* 188:145–156. http://dx.doi.org/10.1083/jcb.200908082

Fernández-Chacón, R., and G. Alvarez de Toledo. 1995. Cytosolic calcium facilitates release of secretory products after exocytotic vesicle fusion. *FEBS Lett.* 363:221–225. http://dx.doi.org/10.1016/0014-5793(95)00319-5

Fisher, R.J., J. Pevsner, and R.D. Burgoyne. 2001. Control of fusion pore dynamics during exocytosis by Munc18. *Science.* 291:875–878. http://dx.doi.org/10.1126/science.291.5505.875

Fulop, T., and C. Smith. 2006. Physiological stimulation regulates the exocytic mode through calcium activation of protein kinase C in mouse chromaffin cells. *Biochem. J.* 399:111–119. http://dx.doi.org/10.1042/BJ20060654

Fulop, T., S. Radabaugh, and C. Smith. 2005. Activity-dependent differential transmitter release in mouse adrenal chromaffin cells. *J. Neurosci.* 25:7324–7332. http://dx.doi.org/10.1523/JNEUROSCI.2042-05.2005

Fulop, T., B. Doreian, and C. Smith. 2008. Dynamin I plays dual roles in the activity-dependent shift in exocytic mode in mouse adrenal chromaffin cells. *Arch. Biochem. Biophys.* 477:146–154. http://dx.doi.org/10.1016/j.abb.2008.04.039

Gong, L.W., G.A. de Toledo, and M. Lindau. 2007. Exocytotic catecholamine release is not associated with cation flux through channels in the vesicle membrane but Na^+ influx through the fusion pore. *Nat. Cell Biol.* 9:915–922. http://dx.doi.org/10.1038/ncb1617

González-Jamett, A.M., X. Báez-Matus, M.A. Hevia, M.J. Guerra, M.J. Olivares, A.D. Martínez, A. Neely, and A.M. Cárdenas. 2010. The association of dynamin with synaptophysin regulates quantal size and duration of exocytotic events in chromaffin cells. *J. Neurosci.* 30:10683–10691. http://dx.doi.org/10.1523/JNEUROSCI.5210-09.2010

González-Jamett, A.M., F. Momboisse, M.J. Guerra, S. Ory, X. Báez-Matus, N. Barraza, V. Calco, S. Houy, E. Couve, A. Neely, et al. 2013. Dynamin-2 regulates fusion pore expansion and quantal release through a mechanism that involves actin dynamics in neuroendocrine chromaffin cells. *PLoS One.* 8:e70638. http://dx.doi.org/10.1371/journal.pone.0070638

Graham, M.E., and R.D. Burgoyne. 2000. Comparison of cysteine string protein (Csp) and mutant α-SNAP overexpression reveals a role for csp in late steps of membrane fusion in dense-core granule exocytosis in adrenal chromaffin cells. *J. Neurosci.* 20:1281–1289.

Grote, E., M. Baba, Y. Ohsumi, and P.J. Novick. 2000. Geranylgeranylated SNAREs are dominant inhibitors of membrane fusion. *J. Cell Biol.* 151:453–466. http://dx.doi.org/10.1083/jcb.151.2.453

Guzman, R.E., Y.N. Schwarz, J. Rettig, and D. Bruns. 2010. SNARE force synchronizes synaptic vesicle fusion and controls the kinetics of quantal synaptic transmission. *J. Neurosci.* 30:10272–10281. http://dx.doi.org/10.1523/JNEUROSCI.1551-10.2010

Haller, M., C. Heinemann, R.H. Chow, R. Heidelberger, and E. Neher. 1998. Comparison of secretory responses as measured by membrane capacitance and by amperometry. *Biophys. J.* 74:2100–2113. http://dx.doi.org/10.1016/S0006-3495(98)77917-2

Han, X., and M.B. Jackson. 2005. Electrostatic interactions between the syntaxin membrane anchor and neurotransmitter passing through the fusion pore. *Biophys. J.* 88:L20–L22. http://dx.doi.org/10.1529/biophysj.104.056739

Han, X., C.T. Wang, J. Bai, E.R. Chapman, and M.B. Jackson. 2004. Transmembrane segments of syntaxin line the fusion pore of Ca^{2+}-triggered exocytosis. *Science.* 304:289–292. http://dx.doi.org/10.1126/science.1095801

Harata, N.C., A.M. Aravanis, and R.W. Tsien. 2006. Kiss-and-run and full-collapse fusion as modes of exo-endocytosis in neurosecretion. *J. Neurochem.* 97:1546–1570. http://dx.doi.org/10.1111/j.1471-4159.2006.03987.x

Hartmann, J., and M. Lindau. 1995. A novel Ca^{2+}-dependent step in exocytosis subsequent to vesicle fusion. *FEBS Lett.* 363:217–220. http://dx.doi.org/10.1016/0014-5793(95)00318-4

He, L., X.-S. Wu, R. Mohan, and L.-G. Wu. 2006. Two modes of fusion pore opening revealed by cell-attached recordings at a synapse. *Nature.* 444:102–105. http://dx.doi.org/10.1038/nature05250

Helfrich, W. 1973. Elastic properties of lipid bilayers: theory and possible experiments. *Z. Naturforsch. C.* 28:693–703. http://dx.doi.org/10.1515/znc-1973-11-1209

Henkel, A.W., H. Meiri, H. Horstmann, M. Lindau, and W. Almers. 2000. Rhythmic opening and closing of vesicles during constitutive exo- and endocytosis in chromaffin cells. *EMBO J.* 19:84–93. http://dx.doi.org/10.1093/emboj/19.1.84

Hille, B. 1992. Ion Channels of Excitable Membranes. Second edition. Sinauer Associates, Inc., Sunderland, MA. 607 pp.

Hua, Y., and R.H. Scheller. 2001. Three SNARE complexes cooperate to mediate membrane fusion. *Proc. Natl. Acad. Sci. USA.* 98:8065–8070. http://dx.doi.org/10.1073/pnas.131214798

Jackson, M.B. 2006. Molecular and Cellular Biophysics. Cambridge University Press, Cambridge. 512 pp. http://dx.doi.org/10.1017/CBO9780511754869

Jackson, M.B. 2007. In search of the fusion pore of exocytosis. *Biophys. Chem.* 126:201–208. http://dx.doi.org/10.1016/j.bpc.2006.05.022

Jackson, M.B. 2009. Minimum membrane bending energies of fusion pores. *J. Membr. Biol.* 231:101–115. http://dx.doi.org/10.1007/s00232-009-9209-x

Jackson, M.B. 2010. SNARE complex zipping as a driving force in the dilation of proteinaceous fusion pores. *J. Membr. Biol.* 235:89–100. http://dx.doi.org/10.1007/s00232-010-9258-1

Jackson, M.B. 2016. The hydrophobic effect in solute partitioning and interfacial tension. *Sci. Rep.* 6:19265. http://dx.doi.org/10.1038/srep19265

Jackson, M.B., and E.R. Chapman. 2006. Fusion pores and fusion machines in Ca^{2+}-triggered exocytosis. *Annu. Rev. Biophys. Biomol. Struct.* 35:135–160. http://dx.doi.org/10.1146/annurev.biophys.35.040405.101958

Jackson, M.B., and E.R. Chapman. 2008. The fusion pores of Ca^{2+}-triggered exocytosis. *Nat. Struct. Mol. Biol.* 15:684–689. http://dx.doi.org/10.1038/nsmb.1449

Jankowski, J.A., T.J. Schroeder, E.L. Ciolkowski, and R.M. Wightman. 1993. Temporal characteristics of quantal secretion of catecholamines from adrenal medullary cells. *J. Biol. Chem.* 268:14694–14700.

Katsov, K., M. Müller, and M. Schick. 2004. Field theoretic study of bilayer membrane fusion. I. Hemifusion mechanism. *Biophys. J.* 87:3277–3290. http://dx.doi.org/10.1529/biophysj.103.038943

Kesavan, J., M. Borisovska, and D. Bruns. 2007. v-SNARE actions during Ca^{2+}-triggered exocytosis. *Cell.* 131:351–363. http://dx.doi.org/10.1016/j.cell.2007.09.025

Khanin, R., H. Parnas, and L. Segel. 1994. Diffusion cannot govern the discharge of neurotransmitter in fast synapses. *Biophys. J.* 67:966–972. http://dx.doi.org/10.1016/S0006-3495(94)80562-4

Klyachko, V.A., and M.B. Jackson. 2002. Capacitance steps and fusion pores of small and large-dense-core vesicles in nerve terminals. *Nature.* 418:89–92. http://dx.doi.org/10.1038/nature00852

Kozlov, M.M., and L.V. Chernomordik. 2015. Membrane tension and membrane fusion. *Curr. Opin. Struct. Biol.* 33:61–67. http://dx.doi.org/10.1016/j.sbi.2015.07.010

Kozlov, M.M., S.L. Leikin, L.V. Chernomordik, V.S. Markin, and Y.A. Chizmadzhev. 1989. Stalk mechanism of vesicle fusion. Intermixing of aqueous contents. *Eur. Biophys. J.* 17:121–129. http://dx.doi.org/10.1007/BF00254765

Kreyszig, E. 1991. Differential Geometry. Dover Publications, New York. 384 pp.

Kwon, S.E., and E.R. Chapman. 2011. Synaptophysin regulates the kinetics of synaptic vesicle endocytosis in central neurons. *Neuron.* 70:847–854. http://dx.doi.org/10.1016/j.neuron.2011.04.001

Lai, Y., J. Diao, Y. Liu, Y. Ishitsuka, Z. Su, K. Schulten, T. Ha, and Y.K. Shin. 2013. Fusion pore formation and expansion induced by Ca^{2+} and synaptotagmin 1. *Proc. Natl. Acad. Sci. USA.* 110:1333–1338. http://dx.doi.org/10.1073/pnas.1218818110

Lam, A.D., P. Tryoen-Toth, B. Tsai, N. Vitale, and E.L. Stuenkel. 2008. SNARE-catalyzed fusion events are regulated by Syntaxin1A–lipid

interactions. *Mol. Biol. Cell.* 19:485–497. http://dx.doi.org/10.1091/mbc.E07-02-0148

Lindau, M., and W. Almers. 1995. Structure and function of fusion pores in exocytosis and ectoplasmic membrane fusion. *Curr. Opin. Cell Biol.* 7:509–517. http://dx.doi.org/10.1016/0955-0674(95)80007-7

Lindau, M., and G. Alvarez de Toledo. 2003. The fusion pore. *Biochim. Biophys. Acta.* 1641:167–173. http://dx.doi.org/10.1016/S0167-4889(03)00085-5

Lindau, M., and E. Neher. 1988. Patch-clamp techniques for time-resolved capacitance measurements in single cells. *Pflugers Arch.* 411:137–146. http://dx.doi.org/10.1007/BF00582306

Lindau, M., B.A. Hall, A. Chetwynd, O. Beckstein, and M.S. Sansom. 2012. Coarse-grain simulations reveal movement of the synaptobrevin C-terminus in response to piconewton forces. *Biophys. J.* 103:959–969. http://dx.doi.org/10.1016/j.bpj.2012.08.007

Lollike, K., N. Borregaard, and M. Lindau. 1995. The exocytotic fusion pore of small granules has a conductance similar to an ion channel. *J. Cell Biol.* 129:99–104. http://dx.doi.org/10.1083/jcb.129.1.99

Lollike, K., N. Borregaard, and M. Lindau. 1998. Capacitance flickers and pseudoflickers of small granules, measured in the cell-attached configuration. *Biophys. J.* 75:53–59. http://dx.doi.org/10.1016/S0006-3495(98)77494-6

Lynch, K.L., R.R. Gerona, D.M. Kielar, S. Martens, H.T. McMahon, and T.F. Martin. 2008. Synaptotagmin-1 utilizes membrane bending and SNARE binding to drive fusion pore expansion. *Mol. Biol. Cell.* 19:5093–5103. http://dx.doi.org/10.1091/mbc.E08-03-0235

MacDonald, P.E., M. Braun, J. Galvanovskis, and P. Rorsman. 2006. Release of small transmitters through kiss-and-run fusion pores in rat pancreatic beta cells. *Cell Metab.* 4:283–290. http://dx.doi.org/10.1016/j.cmet.2006.08.011

Marsh, D. 2006. Elastic curvature constants of lipid monolayers and bilayers. *Chem. Phys. Lipids.* 144:146–159. http://dx.doi.org/10.1016/j.chemphyslip.2006.08.004

Martin, T.F.J. 1994. The molecular machinery for fast and slow neurosecretion. *Curr. Opin. Neurobiol.* 4:626–632. http://dx.doi.org/10.1016/0959-4388(94)90002-7

McMahon, H.T., V.Y. Bolshakov, R. Janz, R.E. Hammer, S.A. Siegelbaum, and T.C. Südhof. 1996. Synaptophysin, a major synaptic vesicle protein, is not essential for neurotransmitter release. *Proc. Natl. Acad. Sci. USA.* 93:4760–4764. http://dx.doi.org/10.1073/pnas.93.10.4760

McNew, J.A., T. Weber, F. Parlati, R.J. Johnston, T.J. Melia, T.H. Söllner, and J.E. Rothman. 2000. Close is not enough: SNARE-dependent membrane fusion requires an active mechanism that transduces force to membrane anchors. *J. Cell Biol.* 150:105–118. http://dx.doi.org/10.1083/jcb.150.1.105

Mellander, L.J., R. Trouillon, M.I. Svensson, and A.G. Ewing. 2012. Amperometric post spike feet reveal most exocytosis is via extended kiss-and-run fusion. *Sci. Rep.* 2:907. http://dx.doi.org/10.1038/srep00907

Michael, D.J., X. Geng, N.X. Cawley, Y.P. Loh, C.J. Rhodes, P. Drain, and R.H. Chow. 2004. Fluorescent cargo proteins in pancreatic beta-cells: design determines secretion kinetics at exocytosis. *Biophys. J.* 87:L03–L05. http://dx.doi.org/10.1529/biophysj.104.052175

Mohrmann, R., H. de Wit, M. Verhage, E. Neher, and J.B. Sørensen. 2010. Fast vesicle fusion in living cells requires at least three SNARE complexes. *Science.* 330:502–505. http://dx.doi.org/10.1126/science.1193134

Monck, J.R., and J.M. Fernandez. 1994. The exocytotic fusion pore and neurotransmitter release. *Neuron.* 12:707–716. http://dx.doi.org/10.1016/0896-6273(94)90325-5

Monck, J.R., G. Alvarez de Toledo, and J.M. Fernandez. 1990. Tension in secretory granule membranes causes extensive membrane transfer through the exocytotic fusion pore. *Proc. Natl. Acad. Sci. USA.* 87:7804–7808. http://dx.doi.org/10.1073/pnas.87.20.7804

Nanavati, C., V.S. Markin, A.F. Oberhauser, and J.M. Fernandez. 1992. The exocytotic fusion pore modeled as a lipidic pore. *Biophys. J.* 63:1118–1132. http://dx.doi.org/10.1016/S0006-3495(92)81679-X

Neco, P., C. Fernández-Peruchena, S. Navas, L.M. Gutiérrez, G.A. de Toledo, and E. Alés. 2008. Myosin II contributes to fusion pore expansion during exocytosis. *J. Biol. Chem.* 283:10949–10957. http://dx.doi.org/10.1074/jbc.M709058200

Neher, E., and A. Marty. 1982. Discrete changes of cell membrane capacitance observed under conditions of enhanced secretion in bovine adrenal chromaffin cells. *Proc. Natl. Acad. Sci. USA.* 79:6712–6716. http://dx.doi.org/10.1073/pnas.79.21.6712

Ngatchou, A.N., K. Kisler, Q. Fang, A.M. Walter, Y. Zhao, D. Bruns, J.B. Sørensen, and M. Lindau. 2010. Role of the synaptobrevin C terminus in fusion pore formation. *Proc. Natl. Acad. Sci. USA.* 107:18463–18468. http://dx.doi.org/10.1073/pnas.1006727107

Nielsen, T.A., D.A. DiGregorio, and R.A. Silver. 2004. Modulation of glutamate mobility reveals the mechanism underlying slow-rising AMPAR EPSCs and the diffusion coefficient in the synaptic cleft. *Neuron.* 42:757–771. http://dx.doi.org/10.1016/j.neuron.2004.04.003

Pawlu, C., A. DiAntonio, and M. Heckmann. 2004. Postfusional control of quantal current shape. *Neuron.* 42:607–618. http://dx.doi.org/10.1016/S0896-6273(04)00269-7

Perrais, D., I.C. Kleppe, J.W. Taraska, and W. Almers. 2004. Recapture after exocytosis causes differential retention of protein in granules of bovine chromaffin cells. *J. Physiol.* 560:413–428. http://dx.doi.org/10.1113/jphysiol.2004.064410

Pieren, M., Y. Desfougères, L. Michaillat, A. Schmidt, and A. Mayer. 2015. Vacuolar SNARE protein transmembrane domains serve as nonspecific membrane anchors with unequal roles in lipid mixing. *J. Biol. Chem.* 290:12821–12832. http://dx.doi.org/10.1074/jbc.M115.647776

Qian, S., W. Wang, L. Yang, and H.W. Huang. 2008. Structure of transmembrane pore induced by Bax-derived peptide: evidence for lipidic pores. *Proc. Natl. Acad. Sci. USA.* 105:17379–17383. http://dx.doi.org/10.1073/pnas.0807764105

Rand, R.P. 1981. Interacting phospholipid bilayers: measured forces and induced structural changes. *Annu. Rev. Biophys. Bioeng.* 10:277–314. http://dx.doi.org/10.1146/annurev.bb.10.060181.001425

Richards, D.A. 2009. Vesicular release mode shapes the postsynaptic response at hippocampal synapses. *J. Physiol.* 587:5073–5080. http://dx.doi.org/10.1113/jphysiol.2009.175315

Richards, D.A., J. Bai, and E.R. Chapman. 2005. Two modes of exocytosis at hippocampal synapses revealed by rate of FM1-43 efflux from individual vesicles. *J. Cell Biol.* 168:929–939. http://dx.doi.org/10.1083/jcb.200407148

Ryham, R.J., M.A. Ward, and F.S. Cohen. 2013. Teardrop shapes minimize bending energy of fusion pores connecting planar bilayers. *Phys. Rev. E Stat. Nonlin. Soft Matter Phys.* 88:062701. http://dx.doi.org/10.1103/PhysRevE.88.062701

Ryham, R.J., T.S. Klotz, L. Yao, and F.S. Cohen. 2016. Calculating transition energy barriers and characterizing activation states for steps of fusion. *Biophys. J.* 110:1110–1124. http://dx.doi.org/10.1016/j.bpj.2016.01.013

Samasilp, P., S.A. Chan, and C. Smith. 2012. Activity-dependent fusion pore expansion regulated by a calcineurin-dependent dynamin-syndapin pathway in mouse adrenal chromaffin cells. *J.*

Neurosci. 32:10438–10447. http://dx.doi.org/10.1523/JNEUROSCI.1299-12.2012

Scepek, S., J.R. Coorssen, and M. Lindau. 1998. Fusion pore expansion in horse eosinophils is modulated by Ca^{2+} and protein kinase C via distinct mechanisms. *EMBO J.* 17:4340–4345. http://dx.doi.org/10.1093/emboj/17.15.4340

Shi, L., Q.T. Shen, A. Kiel, J. Wang, H.W. Wang, T.J. Melia, J.E. Rothman, and F. Pincet. 2012. SNARE proteins: one to fuse and three to keep the nascent fusion pore open. *Science.* 335:1355–1359. http://dx.doi.org/10.1126/science.1214984

Siegel, D.P. 2008. The Gaussian curvature elastic energy of intermediates in membrane fusion. *Biophys. J.* 95:5200–5215. http://dx.doi.org/10.1529/biophysj.108.140152

Sinha, R., S. Ahmed, R. Jahn, and J. Klingauf. 2011. Two synaptobrevin molecules are sufficient for vesicle fusion in central nervous system synapses. *Proc. Natl. Acad. Sci. USA.* 108:14318–14323. http://dx.doi.org/10.1073/pnas.1101818108

Sørensen, J.B. 2009. Conflicting views on the membrane fusion machinery and the fusion pore. *Annu. Rev. Cell Dev. Biol.* 25:513–537. http://dx.doi.org/10.1146/annurev.cellbio.24.110707.175239

Spruce, A.E., L.J. Breckenridge, A.K. Lee, and W. Almers. 1990. Properties of the fusion pore that forms during exocytosis of a mast cell secretory vesicle. *Neuron.* 4:643–654. http://dx.doi.org/10.1016/0896-6273(90)90192-I

Staal, R.G., E.V. Mosharov, and D. Sulzer. 2004. Dopamine neurons release transmitter via a flickering fusion pore. *Nat. Neurosci.* 7:341–346. http://dx.doi.org/10.1038/nn1205

Stiles, J.R., D. Van Helden, T.M. Bartol, E.E. Salpeter, and M.M. Salpeter. 1996. Miniature endplate current rise times less than 100 microseconds from improved dual recordings can be modeled with passive acetylcholine diffusion from a synaptic vesicle. *Proc. Natl. Acad. Sci. USA.* 93:5747–5752. http://dx.doi.org/10.1073/pnas.93.12.5747

Takahashi, N., T. Kishimoto, T. Nemoto, T. Kadowaki, and H. Kasai. 2002. Fusion pore dynamics and insulin granule exocytosis in the pancreatic islet. *Science.* 297:1349–1352. http://dx.doi.org/10.1126/science.1073806

Tanford, C. 1979. Interfacial free energy and the hydrophobic effect. *Proc. Natl. Acad. Sci. USA.* 76:4175–4176. http://dx.doi.org/10.1073/pnas.76.9.4175

Tang, K.S., N. Wang, A. Tse, and F.W. Tse. 2007. Influence of quantal size and cAMP on the kinetics of quantal catecholamine release from rat chromaffin cells. *Biophys. J.* 92:2735–2746. http://dx.doi.org/10.1529/biophysj.106.088997

Taraska, J.W., and W. Almers. 2004. Bilayers merge even when exocytosis is transient. *Proc. Natl. Acad. Sci. USA.* 101:8780–8785. http://dx.doi.org/10.1073/pnas.0401316101

Thomas, L., K. Hartung, D. Langosch, H. Rehm, E. Bamberg, W.W. Franke, and H. Betz. 1988. Identification of synaptophysin as a hexameric channel protein of the synaptic vesicle membrane. *Science.* 242:1050–1053. http://dx.doi.org/10.1126/science.2461586

Trouillon, R., and A.G. Ewing. 2013. Amperometric measurements at cells support a role for dynamin in the dilation of the fusion pore during exocytosis. *ChemPhysChem.* 14:2295–2301. http://dx.doi.org/10.1002/cphc.201300319

Tse, F.W., A. Iwata, and W. Almers. 1993. Membrane flux through the pore formed by a fusogenic viral envelope protein during cell fusion. *J. Cell Biol.* 121:543–552. http://dx.doi.org/10.1083/jcb.121.3.543

Tsuboi, T., and G.A. Rutter. 2003. Multiple forms of "kiss-and-run" exocytosis revealed by evanescent wave microscopy. *Curr. Biol.* 13:563–567. http://dx.doi.org/10.1016/S0960-9822(03)00176-3

van den Bogaart, G., M.G. Holt, G. Bunt, D. Riedel, F.S. Wouters, and R. Jahn. 2010. One SNARE complex is sufficient for membrane fusion. *Nat. Struct. Mol. Biol.* 17:358–364. http://dx.doi.org/10.1038/nsmb.1748

Vardjan, N., M. Stenovec, J. Jorgacevski, M. Kreft, and R. Zorec. 2007. Subnanometer fusion pores in spontaneous exocytosis of peptidergic vesicles. *J. Neurosci.* 27:4737–4746. http://dx.doi.org/10.1523/JNEUROSCI.0351-07.2007

Vardjan, N., M. Stenovec, J. Jorgacevski, M. Kreft, S. Grilc, and R. Zorec. 2009. The fusion pore and vesicle cargo discharge modulation. *Ann. N. Y. Acad. Sci.* 1152:135–144. http://dx.doi.org/10.1111/j.1749-6632.2008.04007.x

Wahl, L.M., C. Pouzat, and K.J. Stratford. 1996. Monte Carlo simulation of fast excitatory synaptic transmission at a hippocampal synapse. *J. Neurophysiol.* 75:597–608.

Walch-Solimena, C., K. Takei, K.L. Marek, K. Midyett, T.C. Südhof, P. De Camilli, and R. Jahn. 1993. Synaptotagmin: a membrane constituent of neuropeptide-containing large dense-core vesicles. *J. Neurosci.* 13:3895–3903.

Wang, C.-T., R. Grishanin, C.A. Earles, P.-Y. Chang, T.F.J. Martin, E.R. Chapman, and M.B. Jackson. 2001. Synaptotagmin modulation of fusion pore kinetics in regulated exocytosis of dense-core vesicles. *Science.* 294:1111–1115. http://dx.doi.org/10.1126/science.1064002

Wang, C.T., J.C. Lu, J. Bai, P.Y. Chang, T.F. Martin, E.R. Chapman, and M.B. Jackson. 2003. Different domains of synaptotagmin control the choice between kiss-and-run and full fusion. *Nature.* 424:943–947. http://dx.doi.org/10.1038/nature01857

Wang, C.T., J. Bai, P.Y. Chang, E.R. Chapman, and M.B. Jackson. 2006. Synaptotagmin-Ca^{2+} triggers two sequential steps in regulated exocytosis in rat PC12 cells: fusion pore opening and fusion pore dilation. *J. Physiol.* 570:295–307. http://dx.doi.org/10.1113/jphysiol.2005.097378

Wang, N., C. Kwan, X. Gong, E.P. de Chaves, A. Tse, and F.W. Tse. 2010. Influence of cholesterol on catecholamine release from the fusion pore of large dense core chromaffin granules. *J. Neurosci.* 30:3904–3911. http://dx.doi.org/10.1523/JNEUROSCI.4000-09.2010

Weiss, A.N., A. Anantharam, M.A. Bittner, D. Axelrod, and R.W. Holz. 2014. Lumenal protein within secretory granules affects fusion pore expansion. *Biophys. J.* 107:26–33. http://dx.doi.org/10.1016/j.bpj.2014.04.064

Wightman, R.M., J.A. Jankowski, R.T. Kennedy, K.T. Kawagoe, T.J. Schroeder, D.J. Leszczyszyn, J.A. Near, E.J. Diliberto Jr., and O.H. Viveros. 1991. Temporally resolved catecholamine spikes correspond to single vesicle release from individual chromaffin cells. *Proc. Natl. Acad. Sci. USA.* 88:10754–10758. http://dx.doi.org/10.1073/pnas.88.23.10754

Wightman, R.M., T.J. Schroeder, J.M. Finnegan, E.L. Ciolkowski, and K. Pihel. 1995. Time course of release of catecholamines from individual vesicles during exocytosis at adrenal medullary cells. *Biophys. J.* 68:383–390. http://dx.doi.org/10.1016/S0006-3495(95)80199-2

Wu, Z., S.M. Auclair, O. Bello, W. Vennekate, N.R. Dudzinski, S.S. Krishnakumar, and E. Karatekin. 2016. Nanodisc-cell fusion: control of fusion pore nucleation and lifetimes by SNARE protein transmembrane domains. *Sci. Rep.* 6:27287. http://dx.doi.org/10.1038/srep27287

Xu, H., M. Zick, W.T. Wickner, and Y. Jun. 2011. A lipid-anchored SNARE supports membrane fusion. *Proc. Natl. Acad. Sci. USA.* 108:17325–17330. http://dx.doi.org/10.1073/pnas.1113888108

Yoo, J., M.B. Jackson, and Q. Cui. 2013. A comparison of coarse-grained and continuum models for membrane bending in lipid bilayer fusion pores. *Biophys. J.* 104:841–852. http://dx.doi.org/10.1016/j.bpj.2012.12.043

Zampighi, G.A., L.M. Zampighi, N. Fain, S. Lanzavecchia, S.A. Simon, and E.M. Wright. 2006. Conical electron tomography of

a chemical synapse: vesicles docked to the active zone are hemifused. *Biophys. J.* 91:2910–2918. http://dx.doi.org/10.1529/biophysj.106.084814

Zhang, Z., and M.B. Jackson. 2008. Temperature dependence of fusion kinetics and fusion pores in Ca^{2+}-triggered exocytosis from PC12 cells. *J. Gen. Physiol.* 131:117–124. http://dx.doi.org/10.1085/jgp.200709891

Zhang, Z., and M.B. Jackson. 2010. Membrane bending energy and fusion pore kinetics in Ca^{2+}-triggered exocytosis. *Biophys. J.* 98:2524–2534. http://dx.doi.org/10.1016/j.bpj.2010.02.043

Zhang, Z., E. Hui, E.R. Chapman, and M.B. Jackson. 2009. Phosphatidylserine regulation of Ca^{2+}-triggered exocytosis and fusion pores in PC12 cells. *Mol. Biol. Cell.* 20:5086–5095. http://dx.doi.org/10.1091/mbc.E09-08-0691

Zhang, Z., E. Hui, E.R. Chapman, and M.B. Jackson. 2010a. Regulation of exocytosis and fusion pores by synaptotagmin-effector interactions. *Mol. Biol. Cell.* 21:2821–2831. http://dx.doi.org/10.1091/mbc.E10-04-0285

Zhang, Z., Z. Zhang, and M.B. Jackson. 2010b. Synaptotagmin IV modulation of vesicle size and fusion pores in PC12 cells. *Biophys. J.* 98:968–978. http://dx.doi.org/10.1016/j.bpj.2009.11.024

Zhao, W.D., E. Hamid, W. Shin, P.J. Wen, E.S. Krystofiak, S.A. Villarreal, H.C. Chiang, B. Kachar, and L.G. Wu. 2016. Hemi-fused structure mediates and controls fusion and fission in live cells. *Nature.* 534:548–552. http://dx.doi.org/10.1038/nature18598

Zhou, P., T. Bacaj, X. Yang, Z.P. Pang, and T.C. Südhof. 2013. Lipid-anchored SNAREs lacking transmembrane regions fully support membrane fusion during neurotransmitter release. *Neuron.* 80:470–483. http://dx.doi.org/10.1016/j.neuron.2013.09.010

Zhou, Z., S. Misler, and R.H. Chow. 1996. Rapid fluctuations in transmitter release from single vesicles in bovine adrenal chromaffin cells. *Biophys. J.* 70:1543–1552. http://dx.doi.org/10.1016/S0006-3495(96)79718-7

Zimmerberg, J., M. Curran, F.S. Cohen, and M. Brodwick. 1987. Simultaneous electrical and optical measurements show that membrane fusion precedes secretory granule swelling during exocytosis of beige mouse mast cells. *Proc. Natl. Acad. Sci. USA.* 84:1585–1589. http://dx.doi.org/10.1073/pnas.84.6.1585

Zimmerberg, J., M. Curran, and F.S. Cohen. 1991. A lipid/protein complex hypothesis for exocytotic fusion pore formation. *Ann. N. Y. Acad. Sci.* 635:307–317. http://dx.doi.org/10.1111/j.1749-6632.1991.tb36501.x